

1-31-1993

Synthesis and characterization of LPCVD boron nitride films for x-ray lithography

Wen-Pin Kuo
New Jersey Institute of Technology

Follow this and additional works at: <https://digitalcommons.njit.edu/theses>



Part of the [Materials Science and Engineering Commons](#)

Recommended Citation

Kuo, Wen-Pin, "Synthesis and characterization of LPCVD boron nitride films for x-ray lithography" (1993).
Theses. 1812.

<https://digitalcommons.njit.edu/theses/1812>

This Thesis is brought to you for free and open access by the Electronic Theses and Dissertations at Digital Commons @ NJIT. It has been accepted for inclusion in Theses by an authorized administrator of Digital Commons @ NJIT. For more information, please contact digitalcommons@njit.edu.

Copyright Warning & Restrictions

The copyright law of the United States (Title 17, United States Code) governs the making of photocopies or other reproductions of copyrighted material.

Under certain conditions specified in the law, libraries and archives are authorized to furnish a photocopy or other reproduction. One of these specified conditions is that the photocopy or reproduction is not to be “used for any purpose other than private study, scholarship, or research.” If a user makes a request for, or later uses, a photocopy or reproduction for purposes in excess of “fair use” that user may be liable for copyright infringement,

This institution reserves the right to refuse to accept a copying order if, in its judgment, fulfillment of the order would involve violation of copyright law.

Please Note: The author retains the copyright while the New Jersey Institute of Technology reserves the right to distribute this thesis or dissertation

Printing note: If you do not wish to print this page, then select “Pages from: first page # to: last page #” on the print dialog screen

The Van Houten library has removed some of the personal information and all signatures from the approval page and biographical sketches of theses and dissertations in order to protect the identity of NJIT graduates and faculty.

ABSTRACT

Synthesis and Characterization of LPCVD Boron Nitride Films for X-ray Lithography

by
Wen-Pin Kuo

Boron nitride thin films were deposited on silicon and fused quartz substrates using ammonia and the liquid precursor borane-triethylamine complex (TEAB) by low pressure chemical vapor deposition over a temperature range of 300-850°C, a pressure range of 0.21-0.6 torr, and an ammonia flow rate range of 0-740 sccm. An increase in the nitrogen content in the film due to the addition of ammonia flow resulted in a pronounced improvement in the optical transmission, an increase in the film uniformity and a decrease in the depletion effect. IR spectra of the films showed an asymmetrical wide band centered around 1400 cm^{-1} and a sharp band around 800 cm^{-1} .

Boron-silicon nitride films were prepared with the incorporation of silicon into the BN films using liquid precursor mixtures consisting of TEAB and hexamethyldisilane (HMDS) at a given temperature, pressure, and ammonia flow rate. The addition of silicon to the films resulted in an achievement of tensile stress and showed an improvement in the mechanical strength of the films. In the IR spectra, two strong absorption peaks centered at 1300 cm^{-1} and 950 cm^{-1} appeared. Boron-silicon nitride membranes, 1 μm in thickness, were successfully made.

**SYNTHESIS AND CHARACTERIZATION OF
LPCVD BORON NITRIDE FILMS
FOR X-RAY LITHOGRAPHY**

**by
Wen-Pin Kuo**

**A Thesis
Submitted to the Faculty of
New Jersey Institute of Technology
in Partial Fulfillment of the Requirements for the Degree of
Master of Science**

Program of Materials Science and Engineering

January, 1993

Blank Page

APPROVAL PAGE

Synthesis and Characterization of
LPCVD Boron Nitride Films
for X-Ray Lithography

Wen-Pin Kuo

Dr. Roland A. Levy, Thesis Advisor
Professor of Physics,
Director of Material Science and Engineering, NJIT

Dr. James M. Grow, Thesis Advisor
Associate Professor of Chemical Engineering, Chemistry, and
Environmental Science, NJIT

BIOGRAPHICAL SKETCH

Author: Wen-Pin Kuo

Degree: Master of Science in Engineering Science

Date: January, 1993

Undergraduate and Graduate Education:

- Master of Science in Engineering Science,
New Jersey Institute of Technology, Newark, NJ, 1993
- Bachelor of Science in Chemical Engineering,
Chinese Culture University, Taipei, Taiwan, 1987

Major: Materials Science and Engineering

ACKNOWLEDGMENT

The author wishes to express his sincere gratitude to his advisors, Professors Roland A. Levy and James M. Grow, for their valuable guidance, inspiration, encouragement and financial support throughout this research, without which it would not have been completed.

Special thanks are due to Dr. Eric Mastromatteo, for his patient guidance, invaluable suggestion, kindness, and friendship during this research work.

The author appreciates the timely help and suggestions from the CVD Lab. members, including Bozena Szkudlarski, Yan-Yao Yu, Wei-Ching Liang, Robert Shih, Vitaly Sigal, Michael Abraizov, Gorthy Chakravarty, Venkat Paturi, and Mahalingam Bhaskaran.

Finally, the author is grateful to his parents H. Y. Kuo and S. P. Kuo, his brother W. K. Guo, and his girl friend Mickey Lin, who encouraged him at every stage of his life.

TABLE OF CONTENTS

Chapter	Page
1 INTRODUCTION.....	1
1.1 Lithography.....	2
1.1.1 Optical Lithography.....	4
1.1.2 X-ray Lithography.....	5
1.1.3 Requirements of X-ray Lithography.....	9
1.2 Chemical Vapor Deposition (CVD).....	11
1.2.1 Fundamental Aspects of CVD.....	12
1.2.2 Low Pressure Chemical Vapor Deposition (LPCVD).....	18
1.2.3 Horizontal Tube LPCVD Reactors.....	19
1.2.4 Advantages of CVD.....	20
1.3 BN Films for X-ray Lithography.....	21
2 EXPERIMENTAL PROCEDURES.....	25
2.1 Introduction.....	25
2.2 LPCVD Apparatus.....	25
2.2.1 Liquid Injection System.....	28
2.3 Experimental Setup.....	30
2.3.1 Leakage Check.....	30
2.3.2 Calibration of Temperature.....	30
2.3.3 Calibration of Gas Flow System.....	31
2.3.4 Calibration of Liquid Injection System.....	34
2.4 Deposition Procedure.....	36
2.5 Preparation of Membranes.....	38
3 EXPERIMENTAL RESULTS AND DISCUSSION.....	39
3.1 Introduction.....	39
3.2 Kinetics of Film Growth.....	40

3.2.1 Effect of Temperature.....	40
3.2.2 Effect of Pressure.....	43
3.2.3 Effect of Ammonia Flow Rate.....	45
3.2.4 Effect of Silicon Additives.....	47
3.3 IR Spectroscopy.....	47
3.4 Refractive Index.....	53
3.5 Density.....	57
3.6 Optical Transmission Spectroscopy.....	57
3.7 Stress.....	62
3.8 Mechanical Properties.....	67
3.9 Annealing Effect.....	74
3.10 Membranes Preparation.....	81
4 CONCLUSIONS.....	82
REFERENCES.....	83

LIST OF TABLES

Table	Page
1.1 Chacters of Borane-Triethylamine Complex (TEAB) and Hexamethyldisilane (HMDS).....	24
3.1 Effect of Temperature on Stress (Without Ammonia)....	65
3.2 Effect of Temperature on Stress (With Ammonia).....	65
3.3 Effect of Ammonia Flow Rate on Stress.....	66
3.4 Effect of Silicon Additives on Stress.....	66
3.5 Effect of Pressure on Stress.....	66

LIST OF FIGURES

Figure	Page
1.1 A Schematic Diagram of Lithography Process.....	3
1.2 Temperature Dependence of Deposition Rate for Typical CVD Films.....	17
2.1 A Schematic Diagram of the LPCVD Reactor.....	26
2.2 A Schematic Diagram of the Liquid Injection System..	29
2.3 Susceptor Temperature Calibration in 40 cm Reaction Zone.....	32
2.4 Susceptor Temperature Calibration at the Center Position of the Furnace.....	33
2.5 Calibration of the Capillary.....	35
3.1 Effect of Temperature on Deposition Rate With no Ammonia.....	41
3.2 Effect of Temperature on Deposition Rate With Ammonia Present.....	42
3.3 Effect of Pressure on Deposition Rate.....	44
3.4 Effect of Ammonia Flow Rate on Deposition Rate.....	46
3.5 Effect of Silicon Additives on Deposition Rate.....	48
3.6 IR Spectrum for Typical BN Films.....	49
3.7 IR Spectrum for BN Films Incorporated With Silicon..	52
3.8 Effect of Temperature on Refractive Index.....	54
3.9 Effect of Ammonia Flow Rate on Refractive Index.....	55
3.10 Effect of Silicon Additives on Refractive Index.....	56
3.11 Effect of Ammonia Flow Rate on Density.....	58
3.12 Effect of Silicon Additives on Density.....	59
3.13 Determination of Optical Transmission.....	61
3.14 Effect of Ammonia Flow Rate on Absorption Coefficient.....	63
3.15 Effect of Silicon Additives on Absorption Coefficient.....	64

3.16	Effect of Temperature on Hardness of BN Films Prepared Without the Use of Ammonia.....	68
3.17	Effect of Temperature on Hardness of BN Films Prepared Using Ammonia.....	69
3.18	Effect of Temperature on Young's Modulus of BN Films Prepared Without the Use of Ammonia.....	70
3.19	Effect of Temperature on Young's Modulus of BN Films Prepared Using Ammonia.....	71
3.20	Effect of Pressure on Hardness.....	72
3.21	Effect of Pressure on Young's Modulus.....	73
3.22	Effect of Ammonia Flow Rate on Hardness.....	75
3.23	Effect of Ammonia Flow Rate on Young's Modulus.....	76
3.24	Effect of Silicon Additives on Hardness.....	77
3.25	Effect of Silicon Additives on Young's Modulus.....	78
3.26	Annealing Effect on the IR Spectra.....	79
3.27	Annealing Effect on the Mechanical Properties.....	80

CHAPTER 1

INTRODUCTION

Microelectronics technology is the basic building-block of many electronic devices such as calculators, computers, telephones, televisions, videos, etc. The most basic of these are integrated circuits, known as chips. Within the last few decades, the microelectronics industry, which has been one of the fastest growing industries, was built-up by the increase in packing density of devices, that is, the ability to fabricate larger number of devices on a single wafer, thus enhancing the performance of the devices. This enhancement in performance added to the higher speed and the lower power consumption gained by the miniaturization of devices in turn leads to reduced cost per function. The search for new techniques, as well as new materials to accomplish this reduction in size, which has now reached the submicron level, has been more and more intensified.

X-ray lithography is a technology that aims at producing miniature devices with submicron feature dimensions. This introduction of x-ray lithography into the microelectronics industry means a revolutionary change in the fabrication technology. However, there is no completely satisfactory source available for a viable x-ray mask, which is a key element to the success of the submicron feature lithography process. Boron nitride with its low atomic number, x-ray and optical transparency, high modulus of

elasticity, and chemical inertness makes it attractive for considered as an x-ray lithography mask material.

The primary goals of this research were to develop a process to deposit boron nitride thin films on silicon substrates using a liquid precursor in a low pressure chemical vapor deposition reactor in order to prepare boron nitride membranes suitable for x-ray lithography masks.

1.1 Lithography

Microcircuit fabrication requires that precisely controlled quantities of impurities be introduced into tiny regions of the silicon substrate, and subsequently these regions must be interconnected to create VLSI circuits. The patterns that define such regions are created by a lithographic process (1).

Lithography is the process of transferring required patterns on a mask to a thin layer of radiation-sensitive material called "resist" which covers the surface of a semiconductor substrate (figure 1.1)(1). The resist, coated as a thin film on the substrate, is subsequently exposed to the radiation through a mask. The mask contains transparent and light-absorbing layers that define the patterns to be created in the resist layer. The areas in the resist exposed to the radiation are made either soluble or insoluble in a specific solvent known as a "developer". A negative resist on exposure to radiation becomes less soluble in a developer solution, while a positive resist becomes more soluble.

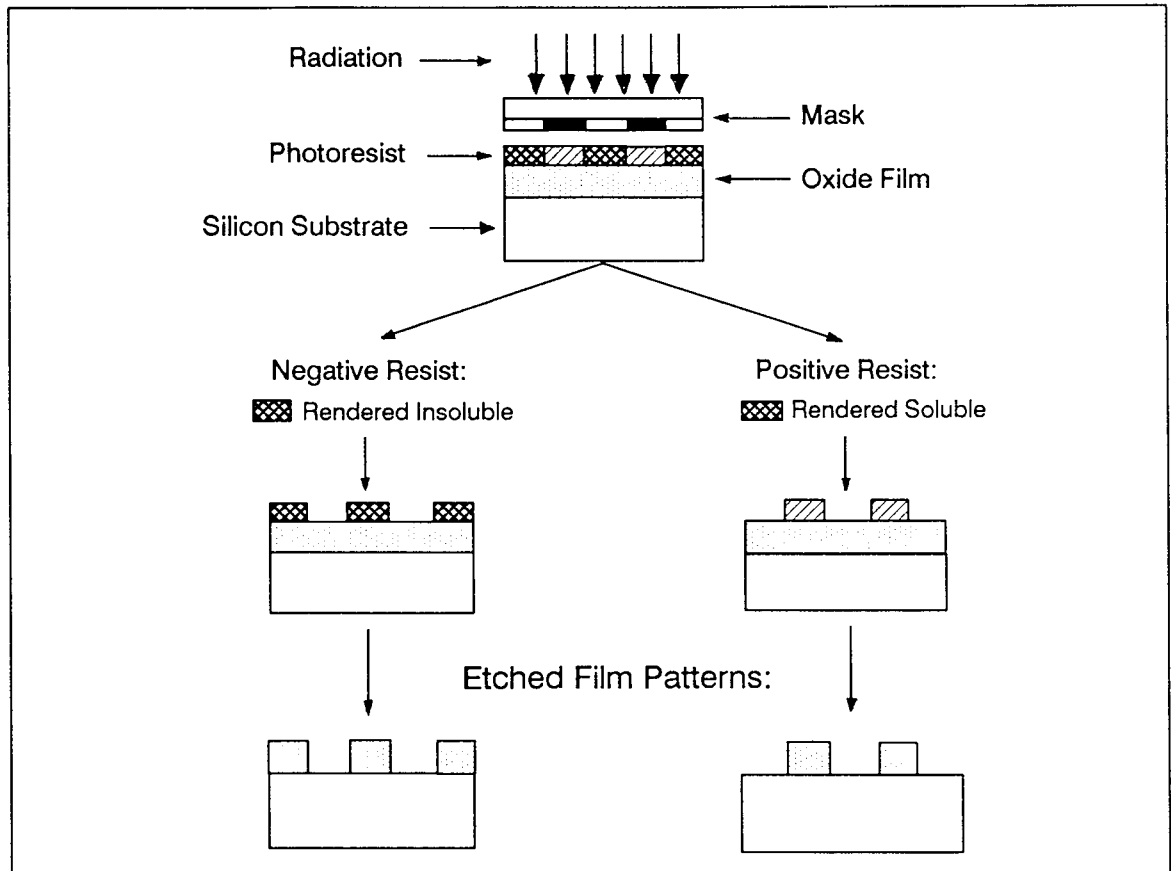


Figure 1.1 A schematic diagram of the lithography process.

Following development, the resist layer no longer covers some regions of the oxide film. The replication of the mask patterns is accomplished by a succeeding etching to these uncovered regions.

A lithographic exposure tool is used to perform the pattern transfer process. The performance of exposure tool is determined by the parameters which include resolution, registration and throughput. Resolution is the minimum feature dimension that can be transferred with high fidelity to the resist layer. Registration is a measurement of how accurately patterns on successive masks can be aligned with respect to the previously defined patterns on the wafer. Most thin film devices require several fabrication steps and the pattern for each step must be accurately positioned with respect to the previous patterns. It is frequently that the overlay accuracy determines the minimum size of the components and not the resolution of the fabrication process. Throughput is the number of wafers that can be exposed per hour.

1.1.1 Optical Lithography

The simplest and most widely used lithographic method in integrated circuit technology is optical lithography. It is comprised the formation of images with ultraviolet radiation (wavelength = 0.2 to 0.4 μm) (2-3) in a photosensitive resist using contact, proximity, or projection printing. Mask consists of a transparent substrate with a thin light-

absorbing layer carrying required patterns. Advantages of optical lithography are (4):

1. Resolution of $0.5 \mu\text{m}$ features over the full field is obtained with routine use, and $0.35 \mu\text{m}$ resolution is attainable under more limited conditions.
2. The effects of high degree of coherence attained with a line narrowed laser.
3. An overlay capability enables it to define a second level pattern on a wafer such that the features register with corresponding features previously defined on wafer.

Limitations of optical lithography are:

1. Exposure times are normally longer.
2. An improvement in the overlay capability is needed.
3. The diffraction effect limits the resolution.

1.1.2 X-ray Lithography

X-ray lithography with wavelengths between 0.2 and 5 nm provides both high-structural resolution as good as $0.1 \mu\text{m}$ and a wide scope of advantages for the application in circuit production (5). It is composed of three elements, the alignment system with an x-ray source, x-ray resist, and x-ray mask (6).

The best radiation quality for x-ray lithography which can be achieved presently is provided by storage rings (5). This so-called synchrotron radiation is emitted by electrons moving with light velocity, which are deflected by a

magnetic field. This radiation is strongly collimated in forward direction; for lithography application it can be assumed to be parallel. Advantages of synchrotron radiation in respect to process performance for semiconductor fabrication are as follows:

1. Parallel radiation which provides x-ray exposure with high depth of focus (several 10 μm) and without any geometrical distortion (blurring, run out) even in the case of mask and wafer unevenness.
2. High intensity up to several 100 mW/cm^2 which allows to utilize medium sensitivity but stable resists for single-layer technique in combination with short exposure time and high throughput.
3. Broadband emission which lowers the Fresnel diffraction, which is also the resolution limiting effect in x-ray lithography.
4. Quasiuniformity in time which is a precondition for an optimal heat dissipation from the mask during exposure.
5. It can have a higher throughput because it uses a parallel exposure.

Based on these facts, there seems to be a worldwide agreement that only synchrotron radiation allows the use of the full scope of advantages of x-ray lithography in semiconductor production. However, problems related to the application of storage rings in lithography are from the huge size of such machines, the inhomogeneous radiation

characteristics in vertical direction to the orbit planes, and the high cost (5).

The mask consists of a transparent substrate with a light-absorbing layer carrying required pattern will be discussed more detail in the following section.

A highly sensitive resist only requires a short exposure which in turn leads to increase the total production rate. Furthermore, high contrast between the exposed and unexposed parts of the resist is required for the pattern to be properly transferred to the resist. The desirable properties of x-ray resist also include high resolution and good resistance to etching agents (4-5).

X-ray lithography is perhaps the most promising method for large-scale production of submicron devices because it offers higher resolution and wider process margins than foreseeable optical cameras and lower cost than scanning electron beams. Advantages of x-ray lithography are (4-6):

1. Much shorter wavelength of x-ray than ultraviolet light reduces the diffraction effect and allowing much higher resolution and non-contact exposure to be achieved simultaneously.
2. Low energy of soft x-rays reduces the scattering effects associated with x-ray absorption within the resist layer.
3. Low absorption of x-rays in the resist material results in uniform, deep exposure and thereby vertical resist profiles.
4. Low particle and dust sensitivity.

5. Replicated linewidth is independent of the substrate material and resist thickness because of the limited scattering, absence of reflection and the uniform exposure.
6. Applicability of simple single-layer resist technique.
7. High depth of focus without any influence of substrate material and chip topography.
8. The highest throughput of all lithography methods which are able to go into the submicron range.

Limitations of x-ray lithography are (4-6):

1. Low intensity of conventional x-ray source results in exposure times on the same order as attainable with advanced direct writing e-beam systems.
2. Complex mask fabrication because it requires the use of mask substrates with thickness in the micron range and it is fragile thus may not be dimensionally stable.
3. Low absorption of x-rays in most resists favors sharp image profiles.
4. Vacuum exposure is needed if x-ray wavelengths above 10 Å are used to achieve very high resolution.
5. Registration methods capable of achieving 0.05 micron are required if the full high resolution capability of the technique is to be exploited.
6. Exposure speed is marginal and that present alignment methods do not offer better accuracy than is achieved with optical lithography.

7. The fabrication of x-ray mother masks by means of e-beam writing and complicated multilevel processes is very expensive and time consuming.

1.1.3 Requirements of X-ray Lithography Mask

The key element for a successful application of x-ray lithography is a well-established and controlled mask technology with respect to accuracy, stability, and nearly zero-defect density. Most efforts in x-ray lithography development are focused on mask technology because this is the field where the final decision for application of x-ray lithography in device fabrication will be made (5). The x-ray mask consists of a thin membrane material with low atomic number carrying a high atomic number absorber pattern, such as gold or tungsten, to provide good pattern definition. The thickness of the supporting membrane depends on its mechanical stability and on both optical and x-ray transparency. The thickness of the absorber ranges between 0.5 and 1.5 μm in order to get a sufficiently high mask contrast. Due to the fact that the carrier membrane has a similar thickness as the absorber, the behavior of the absorber layer severely affects the accuracy and geometrical stability of the entire mask. This problem can only be overcome if the stress of each layer of the mask is compensated or tuned very well. It has to be stable against all environmental influences such as exposure radiation (5).

Suitable membrane material for this technology aimed at providing 0.5-0.2 μm feature dimensions must meet several requirements (1,4-11):

1. High x-ray and optical transmission

Most thin film devices require several fabrication steps and the pattern for each step must be accurately positioned with respect to the previous patterns. More than 50% transmission for x-ray at 6.98 angstroms and optical light at 6328 angstroms wavelength are required.

2. High modulus of elasticity

Higher elasticity increases the ability to withstand the absorber stress and results in a reduction of the membrane thickness or, respectively, a higher mask contrast.

3. Low tensile stress

A small amount of tensile stress is necessary to avoid membrane wrinkling, and to make the absorber free of stress so that there are no distortions due to local variations in absorber coverage.

4. Low surface defect density

5. High radiation hardness (Absence of hydrogen)

The presence of hydrogen in the film generally results in several bonding configurations. Upon irradiation, the bonding configurations of the hydrogen are modified such that the hydrogen becomes weakly bonded. That causes the films to become less tensile, thus resulting in the observed mechanical instability.

6. Uniform thickness

Thickness deviation within 2% in a 2 cm x 2 cm pattern area is required.

7. Easy of fabrication

8. Long lifetime

9. Low cost

The fact that boron nitride films incorporated with silicon offer numerous advantages over several x-ray mask membranes considered made this research very attractive.

1.2 Chemical Vapor Deposition (CVD)

Chemical vapor deposition (CVD) is one of the most important methods of film formation used in the fabrication of very large scale integrated (VLSI) silicon circuits. The main reason for growing thin films by CVD lies in its versatility for depositing a very large variety of materials with excellent step coverage. Another important feature of CVD is the ease for creating films of both homogeneous and graded structures with precisely controllable composition, features that are important in advanced VLSI device fabrication.

Chemical vapor deposition can be defined as a process whereby constituents of the gas or vapor phase react chemically near or on a substrate surface to form a solid product. This product can be in the form of a thin film, a thick coating, or a massive bulk. It can have a single-crystalline, polycrystalline, or amorphous structure. Chemical and physical conditions during the deposition

reaction can strongly affect the composition and structure of the product thus must be understood to control the process. The occurrence of a chemical reaction distinguishes CVD from physical vapor deposition (PVD) processes, such as evaporation and sputtering. This deposition technology has become one of the most important means for creating thin films of solid state microelectronics where some of the most refined purity and composition requirements must be met.

1.2.1 Fundamental Aspects of CVD

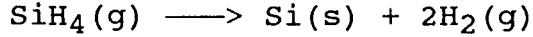
With the increasingly stringent quality requirements imposed on CVD films, a thorough understanding of the underlying principles of this method becomes very important. Since CVD is an interdisciplinary undertaking we shall cross boundaries of several classical fields. First, we shall discuss chemical aspects of CVD. Next, transport phenomena in CVD reactors will be discussed. Finally, the film growth aspects of CVD will be covered briefly.

1.2.1.1 Chemical Aspects of CVD

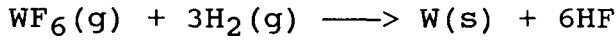
In order to understand CVD processes, we must know which chemical reaction occur in the reactor and to what extent. Furthermore the effects of process variables such as temperature, pressure, input concentrations, and flow rates on these reactions must be studied.

Classification and examples of thermally-activated CVD reaction types are shown as follow (12):

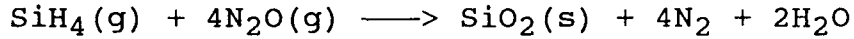
a. Pyrolysis



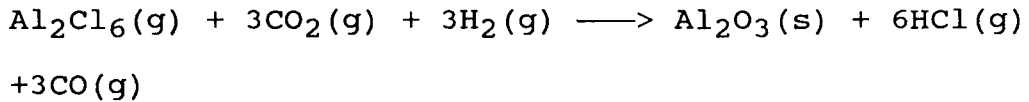
b. Reduction



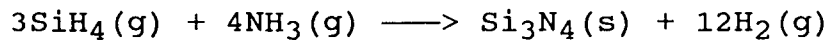
c. Oxidation



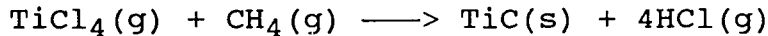
d. Hydrolysis



e. Nitride Formation



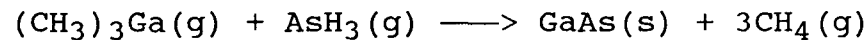
f. Carbide Formation



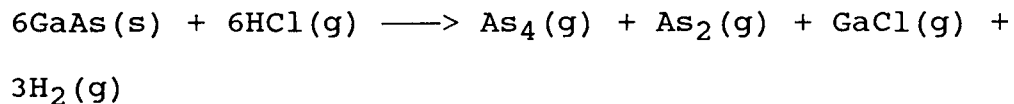
g. Disproportionation



h. Organometallic Reactions



i. Chemical Transport Reaction



The chemical reactions may take place not only on the substrate surface (heterogeneous reaction), but also in the gas phase (homogeneous reaction). Heterogeneous reactions are much more desirable, as such reactions selectively occur only on the heated surfaces, and produce good quality films. Homogeneous reactions, on the other hand are undesirable, as they form gas phase clusters of the depositing material,

which will result in poor adherence, low density, or defects in the film. Thus, one important characteristic of CVD application is the degree to which heterogeneous reactions are favored over homogeneous reactions.

1.2.1.2 Transport Phenomena of CVD

CVD of the film is almost always a heterogeneous reaction. The sequence of steps in the usual heterogeneous processes can be described as follows:

1. Arrival,
 - a. bulk transport of reactants into the chamber,
 - b. gaseous diffusion of reactants to the substrate surface,
 - c. adsorption of reactants onto the substrate surface,
2. Surface events,
 - d. surface diffusion of reactants,
 - e. surface reaction,
3. Removal,
 - f. desorption of by-products from the substrate surface,
 - g. gaseous diffusion of by-products away from the substrate surface,
 - h. bulk transport of by-products out of the reaction chamber.

The steps are sequential and the slowest one is the rate-determining step.

The sequential steps of deposition process can be grouped into 1) mass-transport-limited regime, and 2)

surface-reaction-limited regime. If the deposition process is limited by the mass transfer, the transport process occurred by the gas-phase diffusion is proportional to the diffusivity of the gas and the concentration gradient. The mass transport process which limits the growth rate is only weakly dependent on temperature. On the other hand, it is very important that the same concentration of reactants be present in the bulk gas regions adjacent to all locations of a wafer, as the arrival rate is directly proportional to the concentration in the bulk gas. Thus, to insure films of uniform thickness, reactors which are operated in the mass-transport-limited regime must be designed so that all locations of wafer surfaces and all wafers in a run are supplied with an equal flux of reactant species.

If the deposition process is limited by the surface reaction, the growth rate, R , of the film deposited can be expressed as $R = R_0 * \exp[-E_a/RT]$, where R_0 is the frequency factor, E_a is the activation energy-usually 25-100 kcal/mole for surface process, R is the gas constant, and T is the absolute temperature. In this operating regime, the deposition rate is a strong function of the temperature and an excellent temperature control is needed to achieve the film thickness uniformity required for controllable integrated circuit fabrication. On the other hand, under such conditions the rate at which reactant species arrive at the surface is not as important. Thus, it is not as critical that a reactor be designed to supply an equal flux of

reactants to all locations of a wafer surface. It will be seen that in horizontal LPCVD reactors, wafers can be stacked vertically and at very close spacing because such systems operate in a surface-reaction-rate limited regime. In deposition processes that are mass-transport limited, however, the temperature control is not nearly as critical. As shown in figure 1.2, a relatively steep temperature dependence is observed in the lower temperature range, and a milder dependence in the upper range, indicating that the nature of the rate-controlling step changes with temperature.

1.2.1.3 Film Growth Aspects of CVD

In general, lower temperature and higher gas phase concentration favor formation of polycrystalline deposits. Under these conditions, the arrival rate at the surface is high, but the surface mobility of adsorbed atoms is low. Many nuclei of different orientation are formed, which upon coalescence result in a film consisting of many differently oriented grains. Further decrease in temperature and increase in supersaturation result in even more nuclei, and consequently, in finer-grained films, eventually leading to the formation of amorphous films when crystallization is completely prevented. Amorphous films include oxides, nitrides, carbides, and glasses, are of great technical importance for microelectronics applications.

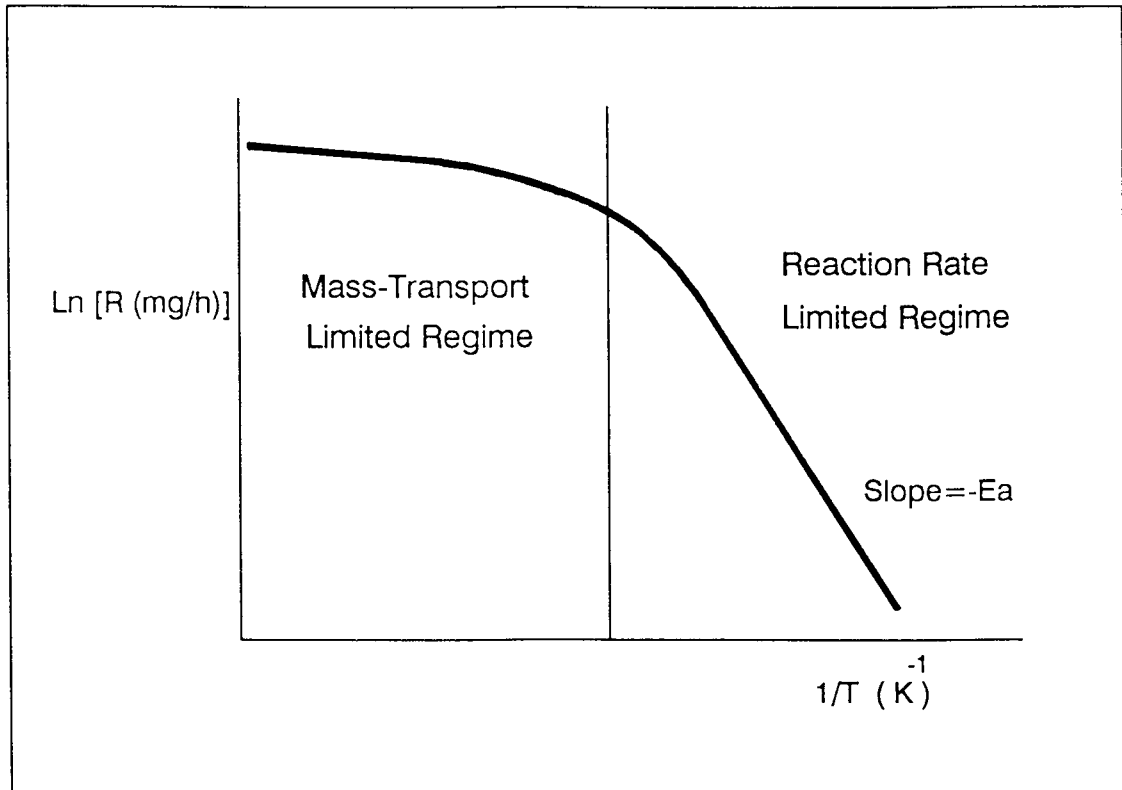


Figure 1.2 Temperature dependence of deposition rate for typical CVD films.

1.2.2 Low Pressure Chemical Vapor Deposition (LPCVD)

The most important and widely used CVD processes are, atmospheric pressure chemical vapor deposition (APCVD), low pressure chemical vapor deposition (LPCVD), and plasma enhanced chemical vapor deposition (PECVD). Only LPCVD is discussed in detail below as this technique was employed in this study.

As discussed before, the deposition rate and uniformity of films created by all CVD processes are governed by 1) the rate of mass transfer of the reactant gases to the substrate surface, and 2) the rate of surface reaction of the reactant gases at the substrate surface. In atmospheric pressure CVD these two rates are usually of the same order of magnitude. Lowering the pressure increases the mean free path of the reactant molecules and also enhances the diffusion of the reactant gas molecules so that mass-transfer to the substrate do not limit the growth rate. The growth rate is limited only by the surface reaction and depends on initial partial pressure of the reactants and temperature. This makes it possible to deposit films uniformly in a highly economical close spaced positioning of the substrate wafers in a stand-up fashion.

LPCVD is able to overcome the uniformity, step coverage, and particulate contamination limitations of APCVD systems (13). It is widely used in the extremely cost competitive semiconductor industry for the deposition of amorphous or polycrystalline films. Two main disadvantages

of LPCVD are the relatively low deposition rate and the relatively high temperature. Attempts to increase deposition rates by increasing the reactant partial pressures tends to initiate gas phase reactions and attempts to operate at lower temperature results in unacceptably slow film deposition.

1.2.3 Horizontal tube LPCVD reactors

Horizontal tube, hot wall reactors are the most widely used LPCVD reactors in VLSI circuit processing for depositing poly-Si, silicon nitride, silicon carbide, boron nitride, and undoped and doped silicon oxide films, etc. In this type of LPCVD reactors, the upright wafers in a carrier boat are radially heated by resistive heating coils surrounding the horizontal quartz tube. Reactant gases are introduced into one end of the tube, and reaction by-products are pumped out from the other end. Vacuum pumps are used to attain the required low deposition pressures. Because of their superior film uniformity, higher wafer throughput, lower production cost, and ability to accommodate larger diameter wafers make this technique very attractive. However, very low deposition rate and sometimes very severe depletion effect in the downstream direction resulting in thinner downstream deposits must be overcome.

1.2.4 Advantages of CVD

Thin films are used in a host of applications in VLSI fabrication, and can be prepared using a variety of techniques. Regardless of the method by which they are formed, however, the process must be economical, and the resultant films must exhibit uniform thickness, high purity and density, controllable composition and stoichiometries, high degree of structural perfection, excellent adhesion, and good step coverage. CVD processes are often selected over competing deposition techniques because they offer the following advantages:

1. A great variety of stoichiometric or nonstoichiometric compositions can be deposited by accurate control of process parameters.
2. High purity films can be deposited that are free from radiation damage without further processing.
3. Results are reproducible.
4. Uniform thickness can be achieved by low pressure.
5. Conformal step coverage can be obtained.
6. Selective deposition can be obtained with proper design of the reactor.
7. The process is very economical because of its high throughput and low maintenance cost.

Technological limitations of CVD include the unwanted and possibly deleterious but necessary by-products of reaction that must be eliminated, and the ever present

1.3 BN Films for X-ray Lithography

The desirable properties of boron nitride thin films such as low density, high thermal conductivity and stability, high electrical resistivity, chemical inertness, corrosion resistance, and desirable mechanical properties make them useful in a wide range of application (14-19). The potential applications of thin boron nitride films which have been proposed include high temperature dielectrics or varistors, heat-dissipation coatings, photoconductors, semiconductor surface protection, boron diffusion sources, diffusion masks, wear-resistant coatings, sodium diffusion barrier and microwave windows (4,9,14,20-22). They have been also considered as membrane materials in x-ray masks used for submicron lithography applications. Such materials must meet several requirements which include high x-ray and optical transmission, high modulus of elasticity, low tensile stress, low surface defect density, radiation hardness, long lifetime, and low cost (6,10).

Because of its technological importance, extensive work has been done to synthesize this material as a thin film. Thin films boron nitride have been grown on various substrates including silicon, quartz, copper, glass, steel, sapphire, tantalum, and fiber (22-23). Boron sources have included diborane, boron trichloride, boron trifluoride, borazine, trichloroborazine, triethyl boron, borane-triethylamine complex, and decaborane (20,24-28). The techniques used have included CVD, plasma enhanced CVD, ion

beams synthesis, pyrolysis, reactive sputtering, e-beam irradiation, ion planting and pulse plasma method (4,9,18-20,22-30). Only diborane-based LPCVD of BN films are discussed in detail because present research is an extended study from it.

Amorphous boron nitride membranes ($4\ \mu\text{m}$ in thickness) produced by LPCVD over the temperature range of $350\text{--}450^\circ\text{C}$ from diborane and ammonia have yielded hydrogenated non-stoichiometric films (6,10,25-26,31-35). These films have been reported to exhibit high x-ray transmission ($\approx 90\%$) at a wavelength of $1\ \text{nm}$ as well as high optical transmission ($\approx 65\%$) at $633\ \text{nm}$. The measured density of such B-H-N films is about $1.7\ \text{g/cm}^3$. The refractive index varied between 1.7 to 3.4 depends on the deposition factors. For the B-H-N structure, the hydrogen content affects the stress and optical transmission. The stress becomes more compressive and the films become optically more transparent as the hydrogen content is increased. At a given temperature, the hydrogen content in the films increases with the ammonia-to-diborane ratio. For a given value of the gas ratio, the hydrogen content decreases with increasing temperature (31-32). Although, a decrease in temperature may lead to increase in optical transmission; unfortunately, this condition lowers the Young's modulus because of excessive hydrogen incorporation. Furthermore, such membranes, which were reproducibly achieved in large areas ($\approx 50\ \text{cm}^2$) with high thickness uniformity (2%) and a low surface defect

density ($\approx 0.1 \text{ cm}^{-2}$) were seen to exhibit a high Young's modulus ($\approx 1.5 \times 10^{11} \text{ Pa}$) and desirable stress values ($5 \times 10^8 \text{ dynes cm}^{-2}$).

The exposure of such films to high synchrotron x-ray frequencies have been shown to result in an enhancement of the surface reactivity to moisture, in a degradation in optical transmission, and in severe instabilities in film stress (10,32-34). These undesirable effects were shown to be attributed to the presence of incorporated hydrogen in the non-stoichiometric $B_xN_yH_z$ compositions. This problem can be resolved by the preparation of stoichiometric BN films under optimized deposition conditions (32).

In addition, using the gas precursor diborane (B_2H_6) as the source of boron for boron nitride films requires expensive cabinets and a cross purging gas supply system for safety reasons. Because this gas is known to be hazardous, toxic, flammable, and explosive. Looking for a safe and economical precursor to deposit excellent performance boron nitride films is one of the primary goal of this research. In this study, an LPCVD process was developed to synthesize amorphous boron nitride films using liquid precursor sources consisting of borane-triethylamine complex (TEAB) and hexamethyldisilane (HMDS). This process also provides the capability of producing as-deposited hydrogen-free films in a temperature regime where depletion effects would preclude the use of diborane. This obviates the need for subsequent high temperature annealing ($\approx 1100^\circ\text{C}$) where phase separation

accompanied with optical and mechanical degradation would normally occur (10,32). Some basic characters of the liquid precursors, TEAB and HMDS, are shown in table 1.1.

Table 1.1 Characters of TEAB and HMDS

Precursors name	Borane-triethylamine complex (TEAB)	Hexamethyldisilane (HMDS)
Chemical Formula	$(C_2H_5)_3N \cdot BH_3$	$(CH_3)_3 \cdot Si \cdot Si \cdot (CH_3)_3$
Molecular Weight (g/mole)	115.03	146.38
Density (g/cc)	0.777	0.729
Melting Point	-4°C	9-12°C
Boiling Point	12 mm/97°C	111-114°C
Color	clear	clear
Flammable	yes	yes

CHAPTER 2

EXPERIMENTAL PROCEDURES

2.1 Introduction

Boron nitride thin films with varying composition were synthesized in a LPCVD reactor with a liquid injection system by adjusting various parameters including temperature, pressure, and reactants nature. IR analysis was carried out to detect the composition of the deposited films, stress of the films was measured and calculated by a laser-beam technique, refractive index and thickness of the films were measured by the ellipsometry and nanospectrometer respectively, mechanical properties of the films were measured using a nanoindenter where as the films optical transmission was measured by the UV-Visible spectrophotometer. Membranes were prepared using a two-step etching technique.

2.2 LPCVD Apparatus

The deposition equipment as shown schematically in figure 2.1 was manufactured by Advanced Semiconductor Materials America, Inc. (ASM America, Inc.) as a Poly Silicon (POLY) micro-Pressure Chemical Vapor Deposition (μ PCVD) system. The reaction took place in a fused quartz process tube with an inside diameter of 13.5 cm and a length of 144 cm. The process tube door was constructed of 300 series stainless steel, had a side hinge, and was sealed by an o-ring. The

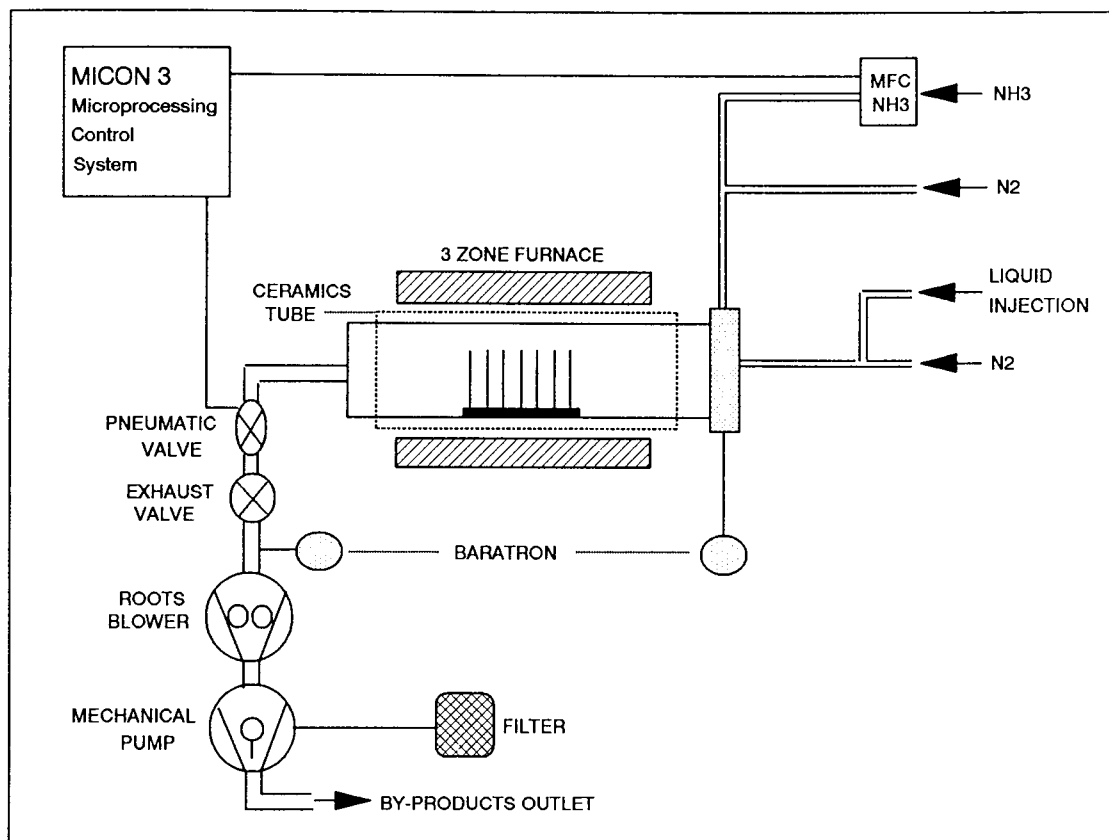


Figure 2.1 A schematic diagram of the LPCVD reactor.

tube door was held closed mechanically and will not open under positive pressure. The process tube was mounted horizontally within a three-zone heating, 10 kwatt, Thermco MB-80 furnace and connected to a vacuum station comprised of a Leybold-Heraeus Trivac dual-stage rotary vane pump model D-60A, backed by a Leybold-Heraeus Ruvac roots pump model WA 250. An oil filter system was used to filter unnecessary particles contamination from ammonia or other reactant by-products and thereby increase the lifetime of the pump. A ceramic tube was setup between the chamber and the heater to enhance the radiation heat transfer thus reduce the temperature deviation through the reaction tube. The furnace temperature was kept constant across all zones and confirmed using a calibrated type K thermocouple. Mass flow controller (ASM inc. model AFC-260) set points were programmed with the MICON 3 microprocessing controller which produces the setpoint voltage and automatically monitors flow vs. programmed flow limits. The reactor pressure was controlled by an automatic exhaust valve and measured at the reactor inlet using a capacitance manometer (13 torr MKS Baratron, type 222B). Separate lines were used for the liquid precursor and the ammonia to prevent the formation of solid compounds in the gas line. Silicon wafers stood vertically on a fused quartz boat, perpendicular to the reactant flow, with a 2 cm spacing between adjacent wafers.

2.2.1 Liquid Injection System

The injector, designed and fabricated in-house, consisted of a stainless steel bubbler connected to a pre-calibrated capillary tube fastened onto the reaction chamber. The liquid flow rate through the injector was established at different pressure differentials and for various capillary tube geometries. The flow rate is inversely proportional to the length of the capillary, while proportional to the pressure differential and the cross-sectional area. A schematic diagram of this injection system, which included filters for both nitrogen purge (140 μm) and liquid precursor (7 μm) to reduce capillary blockage, is shown in figure 2.2. The metal bubbler was filled with the amount of liquid precursor required for a given experiments and pressurized with nitrogen for keeping a positive pressure to restrict oxygen leak into it. This should be handled in an inert glove box because the liquid precursor can slowly react with humidity and form undesirable white powder contamination. Additionally, a separate steady flow of 60 sccm of N_2 was used as a carrier gas to facilitate the evaporation and transport of the precursor at the capillary end into the reaction chamber. Except where noted, the flow rate of the TEAB complex was kept at 17 sccm using a pressure of 6 psi gauge throughout these experiments.

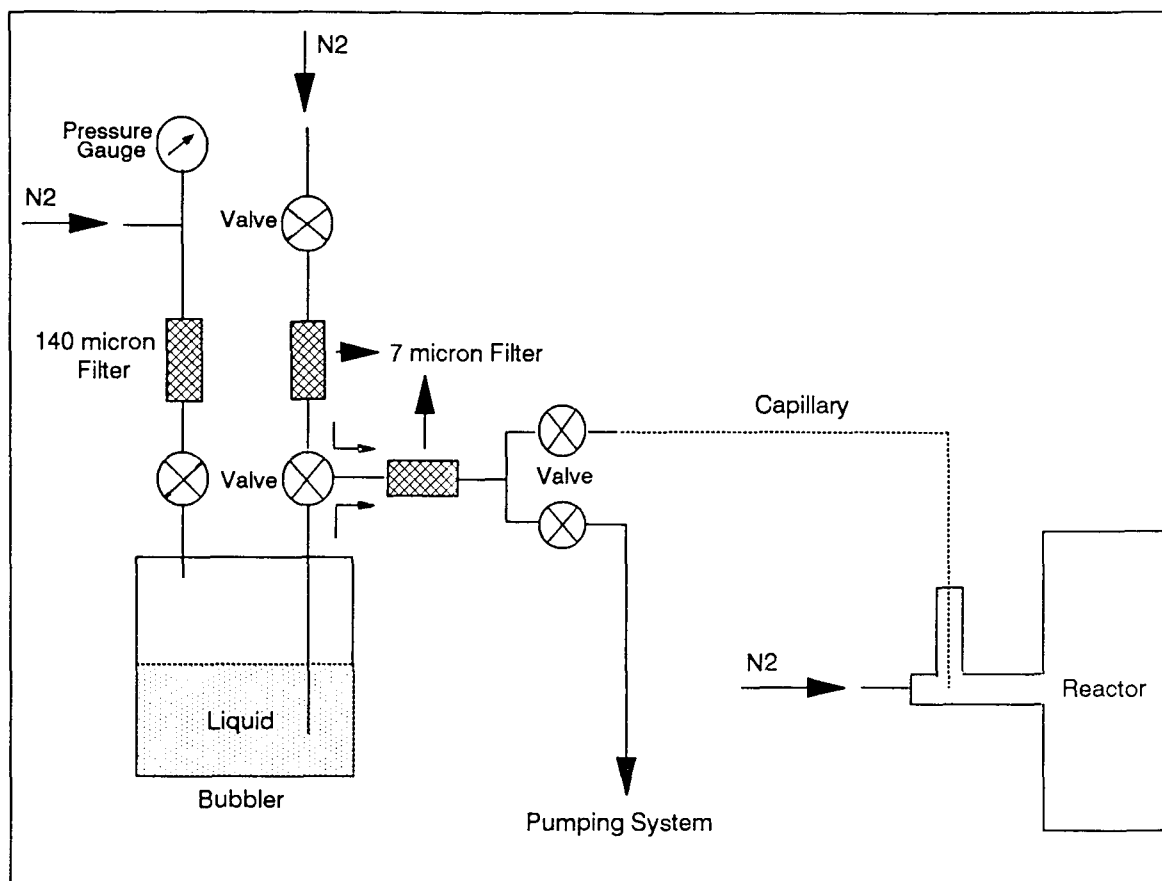


Figure 2.2 A schematic diagram of the liquid injection system.

2.3 Experimental Setup

2.3.1 Leakage Check

A leak would result in a change in the deposit structure (due to oxygen) and could result in haze depending on the size of the leak, therefore a leakage check in the CVD setup is an important step before making an experiment (36). When carrying out leakage check, all pneumatic valves, mass flow controllers, and gas regulators should be fully open to the gas cylinder main valves. The capillary is disconnected and the inlet is sealed with a plug because it is not possible to create a vacuum in the capillary in limited time period. After pumping the reaction system for a whole day, closing the outlet valve of the chamber, the pressure increasing rate was measured at a fixed period of time in the chamber to obtain the leakage rate. For this LPCVD system, the leakage rate deviated between 0.13 to 2 mtorr/minute depending on the chamber condition. A very low leakage rate for a new chamber and a much higher leakage rate for chamber after long time in service. However, the leakage rate in this system was basically good.

2.3.2 Calibration of Temperature

A calibrated type thermocouple served to confirm the exact temperature of the reaction chamber and introduced from a inlet on the door into the chamber. For the safety reason, calibrating susceptor temperature started from a low

setpoint and was raised step by step. Waiting for one hour for the temperature to increase from room temperature to the first setup temperature was necessary to equilibrate the susceptor temperature. An additional thirty minutes was necessary to increase the temperature to each successive setpoint. Seven points within a 40 cm reaction zone near the furnace center were calibrated as shown in figure 2.3. Ten minutes at each point was required to equilibrate the temperature. Furthermore, the center position of the reaction zone was designed to be the setpoint temperature theoretically and the calibrated results are plotted in figure 2.4.

2.3.3 Calibration of Gas Flow System

The flow rates for the reactant gas (NH_3) and the inert gas (N_2) were calibrated by the same means. Using the Ideal Gas Law, $PV = nRT$, the following formula was developed to calibrate the flow rate:

$$\frac{dV}{dt} = \frac{V_R}{760} \times \frac{273}{T_m} \times \frac{dP}{dt}$$

where dV/dt is the flow rate of the tested gas in sccm, V_R is the pre-calculated volume of reactor ($20,900 \pm 600 \text{ cm}^3$), T_m is the measured chamber temperature in Kelvin, and dp/dt is the rate of pressure increase. The tested gas in the vacuum condition is considered as an ideal gas and the reaction chamber was evacuated for several hours prior to testing. After setting the set-up flow rate, gas line was

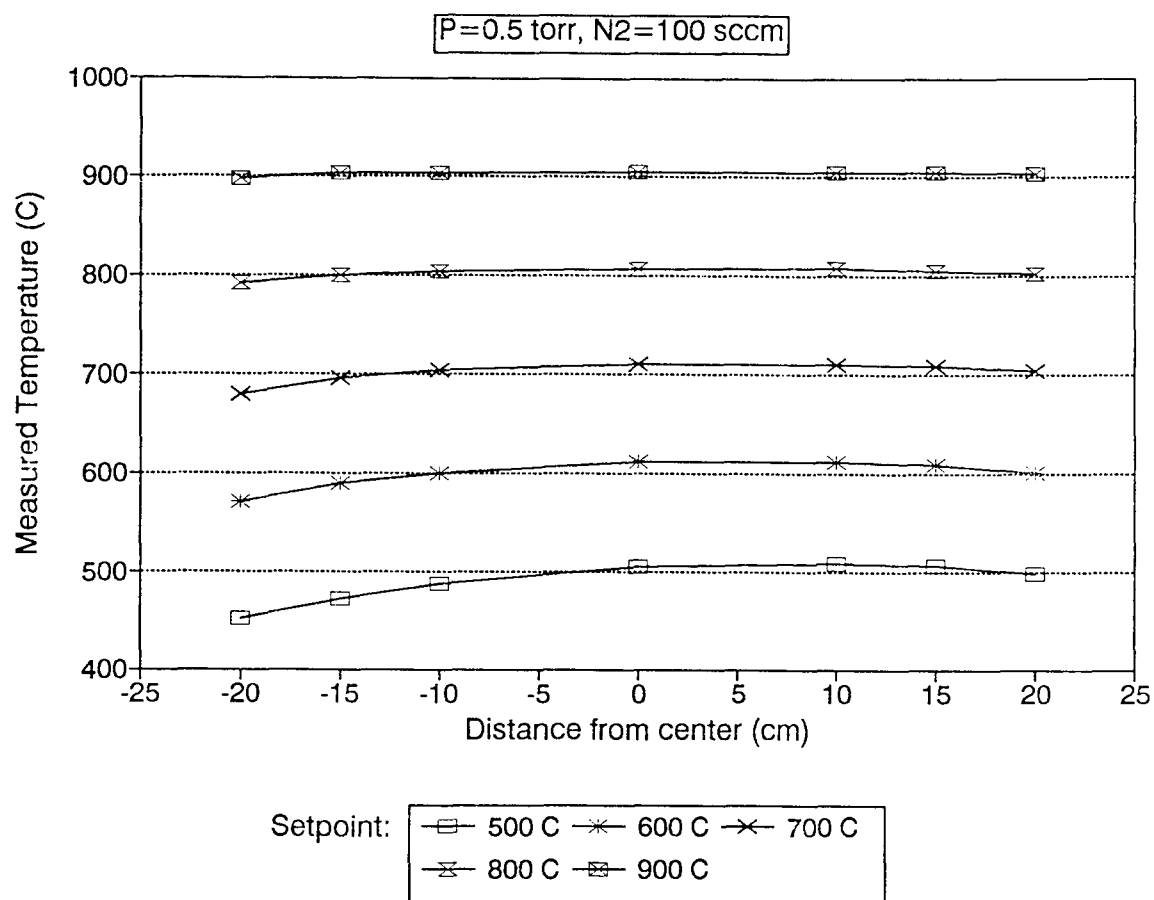


Figure 2.3 Susceptor temperature calibration of the reaction chamber over a 40 cm reaction zone at a constant pressure of 0.5 torr and N₂ flow rate of 100 sccm.

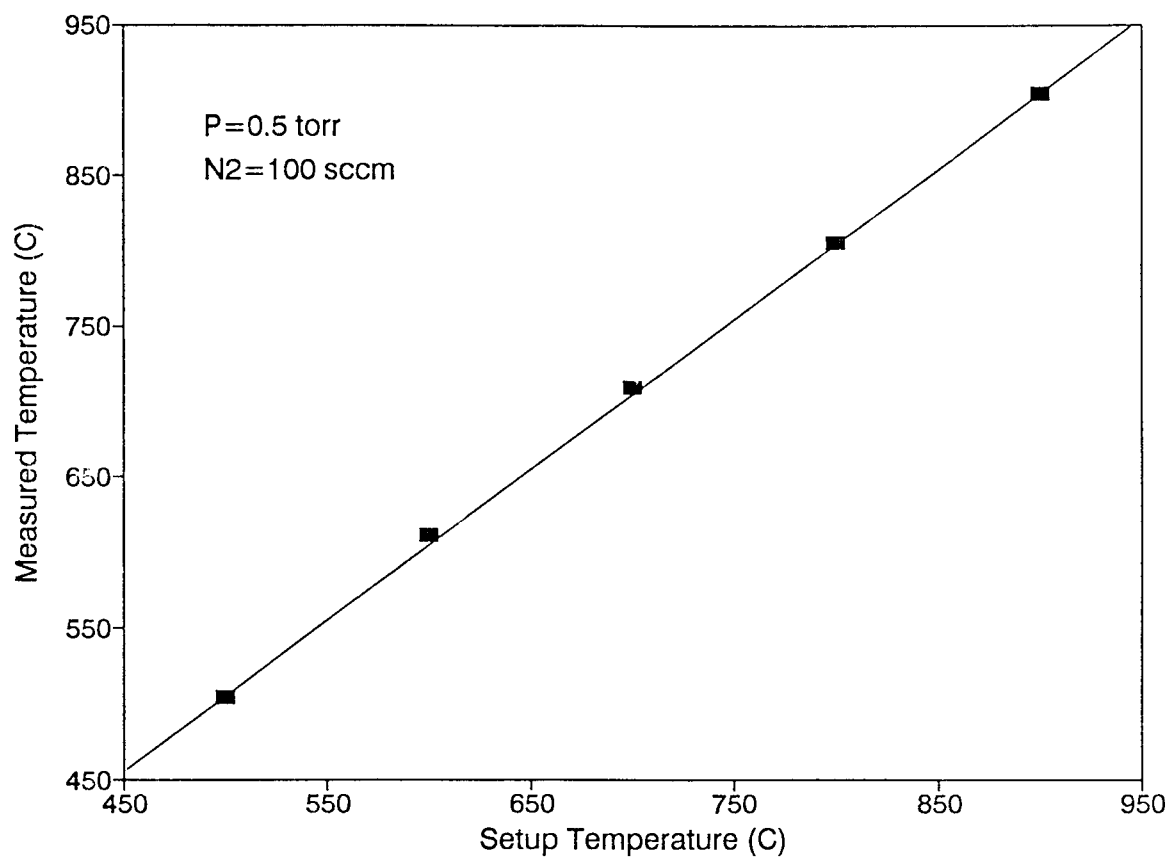


Figure 2.4 Susceptor temperature calibration for the center position of the furnace at a constant pressure of 0.5 torr, and N₂ flow rate of 100 sccm.

opened to introduce the gas flow into the chamber, then the outlet valve of the chamber was closed and the pressure difference in the chamber was measured to obtain the rate of pressure increase. The real flow rate of the tested gas thus can be calculated. The accuracy of this calibration involves the gas flow rate, the time interval, and the condition of the chamber should be carefully controlled. A smaller gas flow rate causes a slower pressure increasing rate in turn leads to an easier detection on the pressure increase and more accurate calibration. A longer time interval for calibration and a good vacuum condition in the chamber are also favored in the accuracy of calibration.

2.3.4 Calibration of Liquid Injection System

Since the vapor pressure of the TEAB complex is very low (12 torr at 97°C), it is difficult to obtain a flow rate by the previous method. Therefore, another calibration process was developed to calibrate the liquid precursor flow rate. By collecting the liquid from the capillary end and measuring the weight of the liquid at a fixed pressure drop so that the weight consumed per minute at this fixed pressure drop was determined. The Ideal Gas Law was used to calculate the vapor volume which could be produced at STP in order to obtain a result in the units of sccm. Figure 2.5 presents a calibrated TEAB flow rate as a function of the pressure drop through the capillary (0.01 inch in inside diameter and 550 cm in length). For a constant pressure drop of 20.7 psi (6

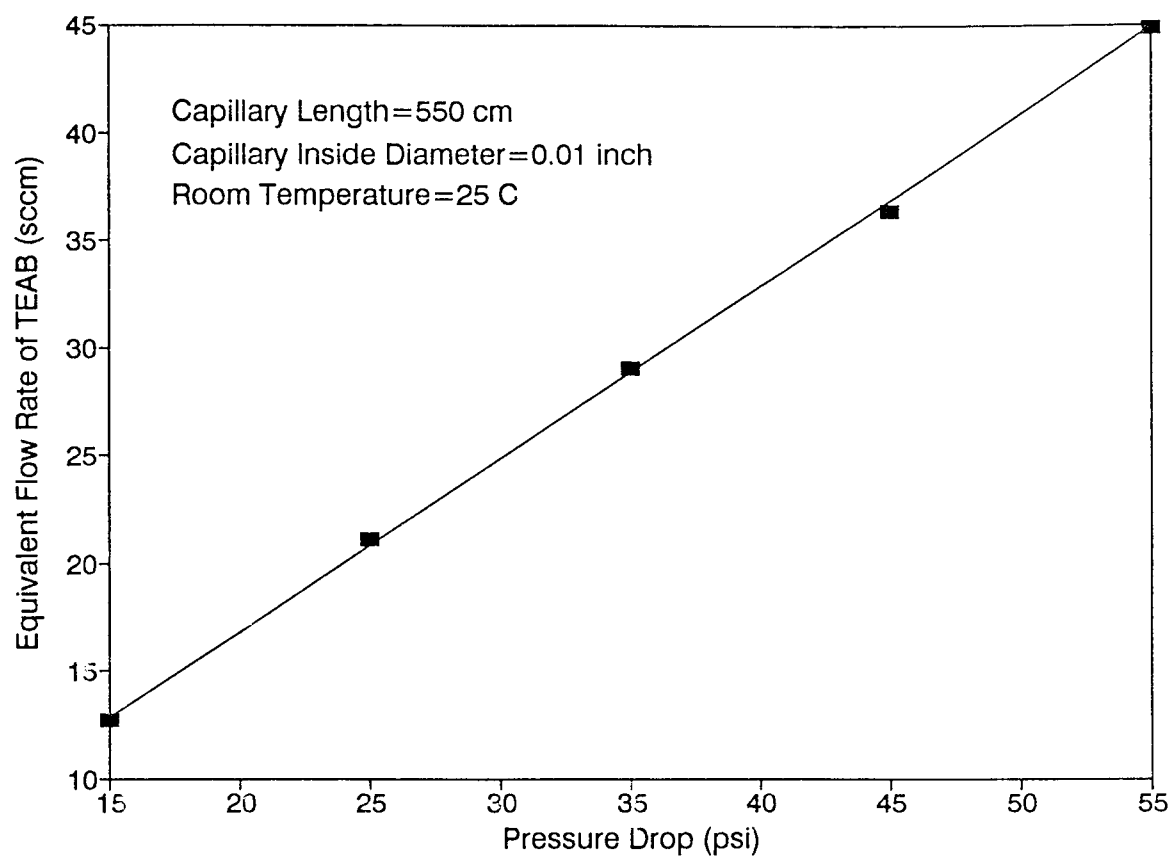


Figure 2.5 Calibration of capillary (0.01" in inside diameter, 550 cm in length) flow rate as a function of pressure drop.

psi gauge pressure attached to the bubbler), the flow rate of TEAB is shown to be about 17 sccm. A calibration of capillary before each experiment is important to ensure that the capillary is in good working condition confirming that the amount of deposits can be precisely controlled. This can be performed by introducing a constant pressure of N_2 flow through the capillary into the isolated chamber, then measuring the rate of pressure increase to compare with a previous rate of pressure increase.

2.4 Deposition Procedure

Boron nitride films deposited on p-type, boron-doped, single-side polished $\langle 100 \rangle$ silicon wafers (Silicon Sense Inc., 10 cm in diameter, 525 μm in thickness), and fused silica quartz wafers (Hoya, Japan) were placed in an upright position on a fused quartz boat and spaced 2 cm apart. Eight wafers were used for each experiment. Two dummies, three $\langle 100 \rangle$ oriented silicon samples, and one quartz wafer were put on the single slots of the loading boat. One stress monitor, $\langle 100 \rangle$ oriented silicon, and one $\langle 111 \rangle$ oriented silicon were put back to back on the double slot of the boat. The mass of deposit was accurately weighed to 0.1 mg by a four decimals electronic balance before and after experiment. The boat was placed in the reaction chamber at a distance of 58 cm from the loading end thereby placing the third double slot positioned on the exact center of the chamber, thus wafers were center-distributed from this

point. In order to have an uniform deposition temperature within the reaction zone, heating the chamber for at least one hour before starting experiment is necessary especially for a lower temperature (i.e. lower diffusion) experiment. Deposition time was varied according to the film thickness requirement. Samples were cooled to room temperature in the vacuum environment for about five hours before removed for analysis.

The deposition rates were obtained by measuring the mass of deposits for a known time interval, in units of mg/hr. The IR spectra were taken using a Perkin Elmer IR Spectrophotometer 580 to detect the composition of films while the UV/visible data were taken with a Varian DMS 300 Spectrophotometer to inspect the optical transmission of films. The thickness and the refractive index were measured by the Rudolph Research/Autdec ellipsometry and the Nanometrics NanoSpec/AFT nanospectrometer. The hardness and Young's modulus of the films were determined using a Nano Instruments indenter. The stress of the films was measured using a home-made optically laser-beam equipment. With this technique, the radius of curvature was measured before and after the deposition of the film and the change in the radius of curvature is ascribed to the stress of the film. Thin wafers were preferred so that the stresses could be measured more accurately (25-26).

2.5 Preparation of Membranes

A two-step process was used to prepare membranes. Using an aluminum shadow mask, the film was dry etched from the backside of the wafer exposing the silicon substrate to a plasma environment for twenty minutes. The plasma produced was created from the AMP 3300 2A PECVD reactor system, using constant flow of CF_4 (80 sccm) and O_2 (360 sccm) in a total pressure of 200 mtorr, and an RF power of 500 watt. After removing the exposed part of the film, the silicon wafer was then chemically etched in a heated KOH solution bath (Baker Analyzed, Potassium Hydroxide 45.8% solution), to remove the exposed silicon. It takes about 6 hours to dissolve the exposed silicon (525 μm in thickness) in an 80°C, 25% concentration KOH solution. The KOH solution was diluted by the stiller water. A very gentle action is required to treat on the submicron feature membranes.

CHAPTER 3

EXPERIMENTAL RESULTS AND DISCUSSION

3.1 Introduction

The properties required of membrane materials for x-ray masks useful in submicron lithography application include high x-ray and optical transmission, low tensile stress, high modulus of elasticity, absence of hydrogen, uniform thickness, low surface defect density, and long life time. To develop a LPCVD boron nitride process, the parameters that effect the composition and properties of the films were studied including the follows:

1. deposition temperature,
2. deposition pressure,
3. ammonia flow rate,
4. silicon additives.

These deposition variables are so many and complex, trying to reach an ideal deposition condition for creating satisfactory membranes suitable for x-ray lithography mask substrates was very difficult. Therefore, the depositions were done in very carefully controlled experiments. There were 46 experiments for this research. The boron nitride films were deposited at a fixed precursor flow rate of 17 sccm, a temperature range of 300 to 850°C, a pressure range of 0.21 to 0.6 torr, and a ratio of ammonia/liquid precursor flow range of 0 to 44. The precursor mixture consisting of HMDS and TEAB was varied in the ratio range of 1/25 to 1/3.

3.2 Kinetics of Film Growth

The films produced through the use of the TEAB complex as a sole precursor were first investigated. At a fixed precursor flow rate of 17 sccm and total pressure of 0.5 torr, the deposition rate as a function of deposition temperature in the range of 600 to 850°C are shown in figure 3.1. There was almost no deposition below 550°C. From 600 to 800°C, the deposition rate followed an Arrhenius behavior yielding an apparent activation energy of 11 kcal/mole. Above 800°C, the deposition rate was observed to decrease with increasing temperature due to the depletion effects caused by the increased rate of side reactions in the gas phase and the associated reduction in the amount of material available for substrate surface reactions.

Films deposited with no ammonia were found to be dark in all cases because of the high boron and carbon content. Ammonia was added to the boron precursor in order to increase the nitrogen content and decrease the boron and carbon content in the films. The deposition rates were determined as a function of temperature, pressure, NH₃ flow rate, and HMDS/TEAB ratio.

3.2.1 Effect of Temperature

At a fixed total flow rate of 187 sccm, NH₃/TEAB ratio of 10/1 and total pressure of 0.5 torr, the kinetics of film growth were investigated in the temperature range of 300 to 850°C and shown in figure 3.2. The deposition rate plotted

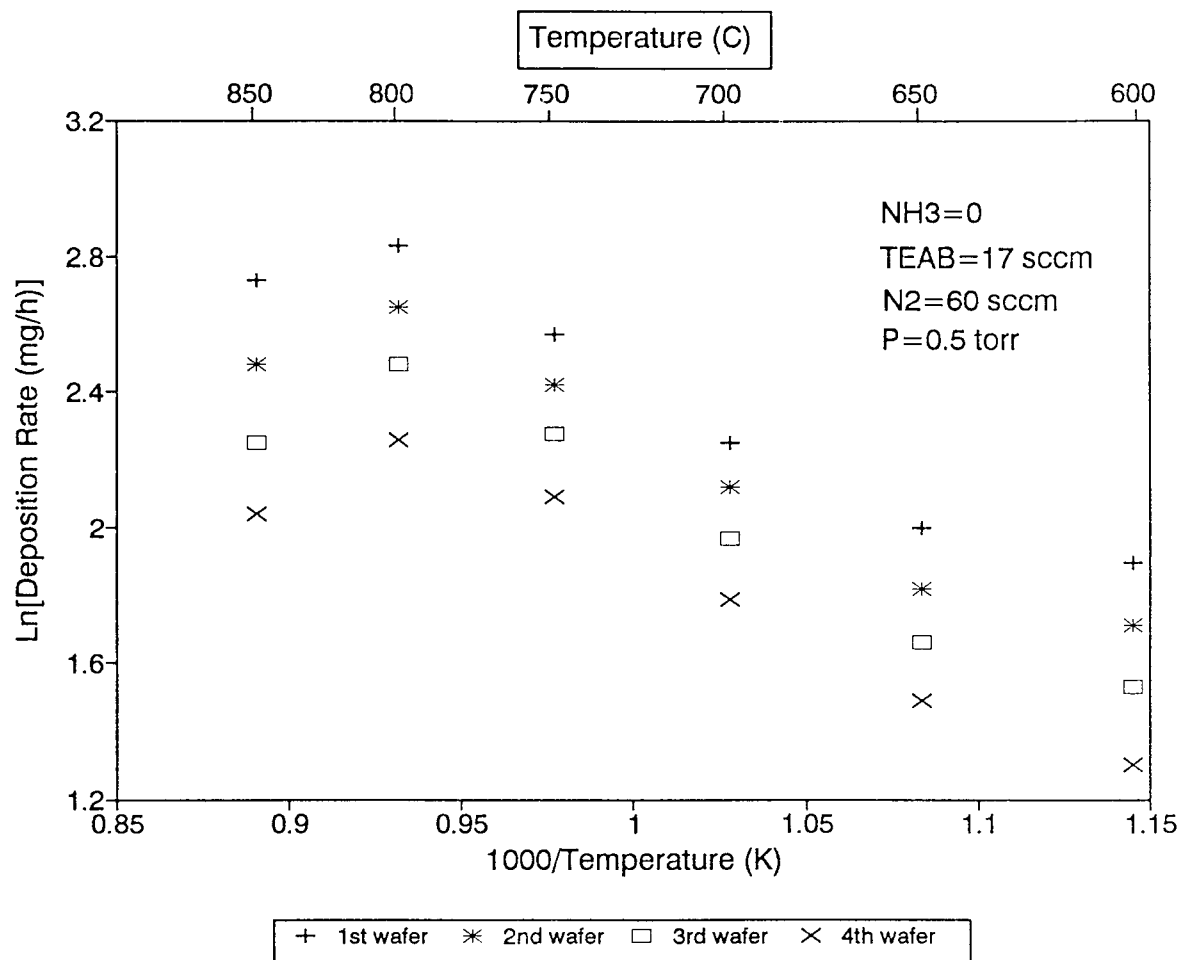


Figure 3.1 Effect of temperature on deposition rate with no ammonia at a constant pressure of 0.5 torr, TEAB flow rate of 17 sccm, and N₂ flow rate of 60 sccm.

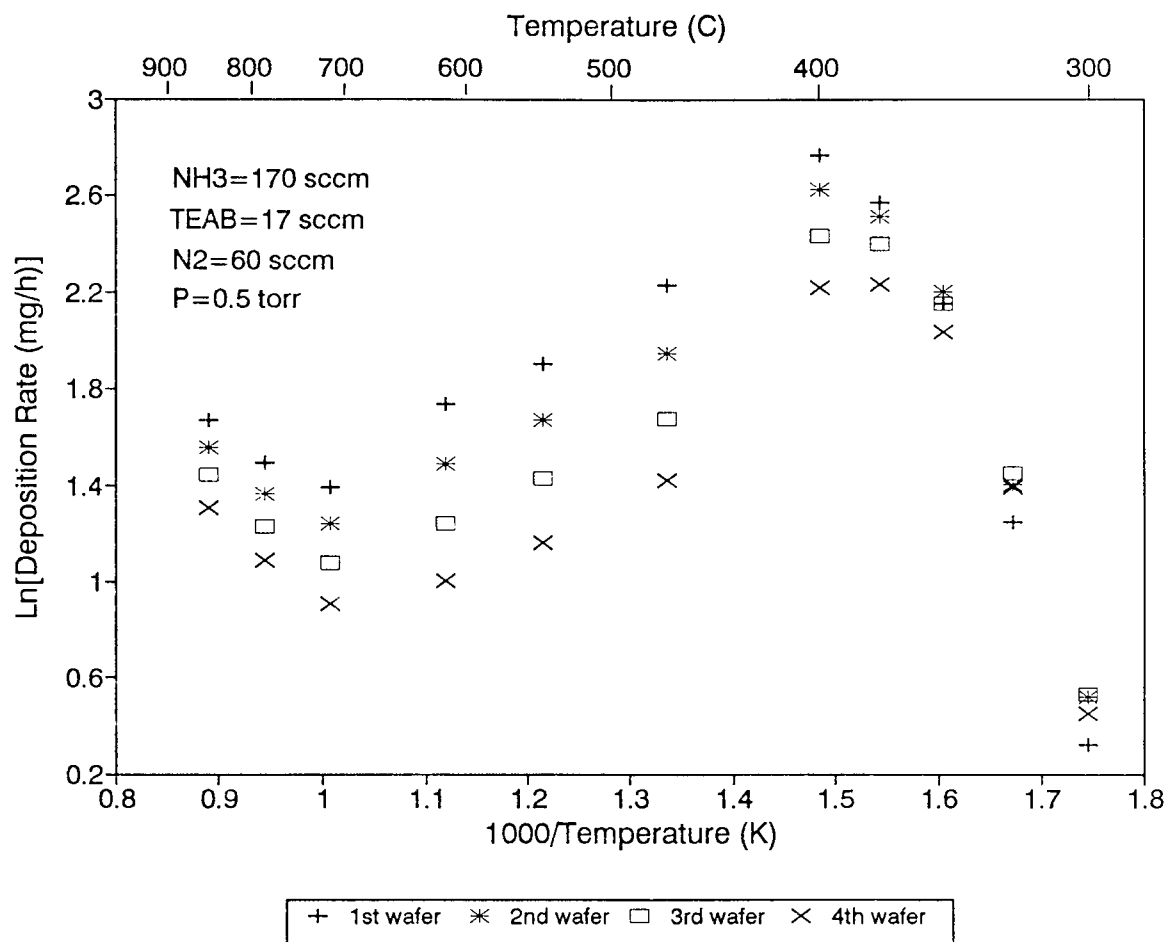


Figure 3.2 Effect of temperature on deposition rate with ammonia present at a constant pressure of 0.5 torr and TEAB flow rate of 17 sccm.

over the range of 300 to 350°C exhibits an Arrhenius behavior with an activation energy of 22 kcal/mole. The addition of NH₃ had the effect of lowering the minimum deposition temperature by around 300°C. Between 350 and 400°C, the curve changes slope reflecting the onset of the changes in reaction mechanism. It was observed that at these low temperature region, the reactants did not become sufficiently hot prior to their flow over the substrates; as they travel toward the exhaust they become warmer leading to increased deposition rates on the last wafer along the flow. In the range between 400 to 700°C, the deposition rate decreases monotonously due to the increased contribution of depletion effect. Above 720°C, the slight increase in deposition rate is assumed to be due to changes in the gas phase chemistry which are also reflected in the changes in the film composition, density, stress, color, etc. The films become dark after this temperature and the stress changes from tensile to compressive. The general shape of this curve is complex and generally consistent to the curve of the refractive index measurement (refer to figure 3.8, page 54) reflecting the chemical mechanism of the processes and the composition of the films are strongly dependent on the temperature.

3.2.2 Effect of Pressure

The effect of pressure on deposition rate is shown in figure 3.3 for constant conditions of temperature (850°C) and

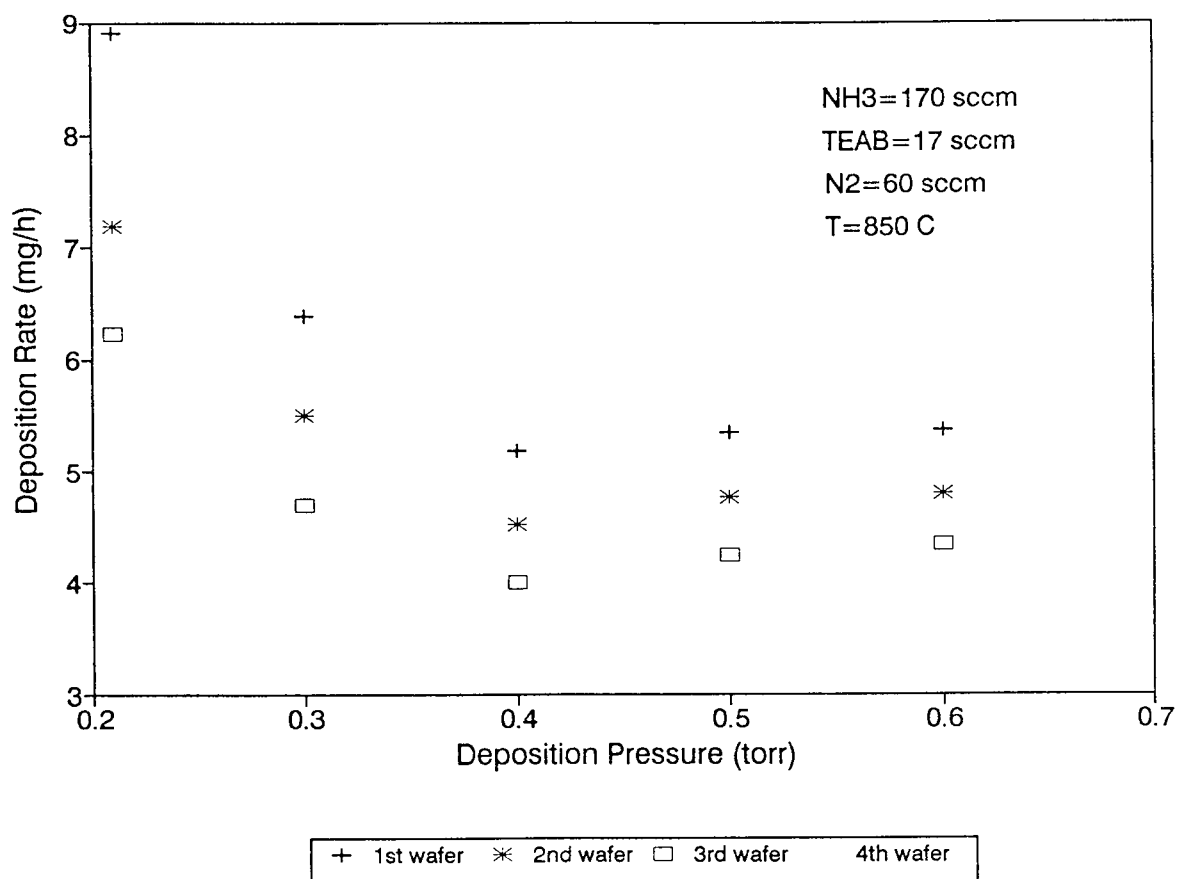


Figure 3.3 Effect of pressure on deposition rate for the reaction between NH₃ and TEAB complex at a constant temperature of 850°C.

NH₃/TEAB ratio (10/1). Although little change in deposition rate is seen above 0.4 torr, there is a marked increase in the rate at lower pressures. This increase may be associated with an increased dissociation of the borane complex at lower pressures or an increased removal of inhibiting by-products from the substrate surface at the increased pumping rate necessary to obtain the lower pressure.

3.2.3 Effect of Ammonia Flow Rate

Figure 3.4 illustrates the dependence of deposition rate on NH₃ flow rate in the range of 0 to 740 sccm for a given TEAB flow rate of 17 sccm, temperature of 850°C, and total pressure of 0.5 torr. As the NH₃ flow rate increases, the deposition rate decreases rapidly approaching a plateau after around 350 sccm with an accompanying improvement in the depletion effect. The deposition rate from wafer to wafer across a 8 cm reaction zone shows less than 5% deviation. Both these observations can be explained by considering the dilute effect of the complex precursor because the increase in the NH₃ flow must be compensated at constant total pressure by an increase in pumping speed that causes a reduction in the precursor partial pressure. The nitrogen content increases with the addition of NH₃ flow also contributing to a more stoichiometric BN film.

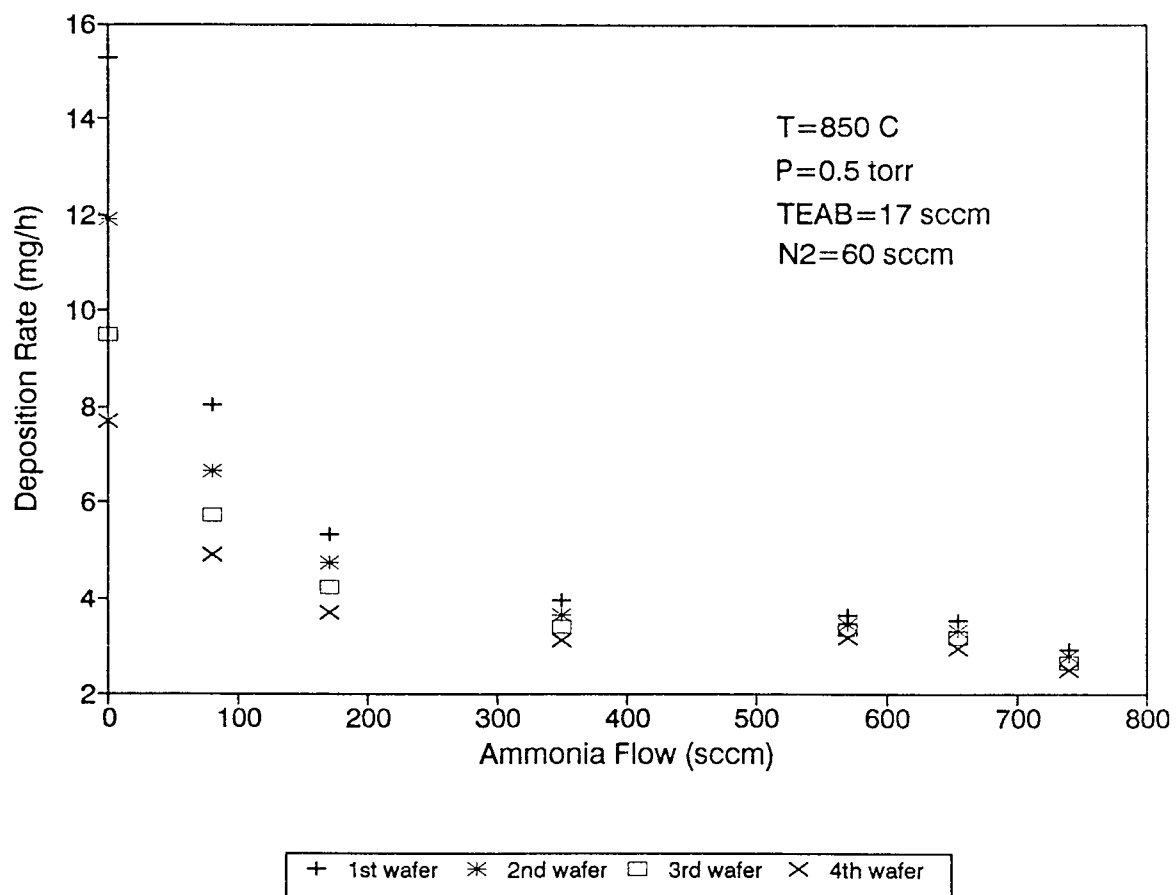


Figure 3.4 Effect of ammonia flow rate on deposition rate for the reaction between NH_3 and TEAB complex at a constant temperature of 850°C and pressure of 0.5 torr.

3.2.4 Effect of Silicon Additives

At a fixed temperature of 850°C, total pressure of 0.5 torr, and ammonia flow rate of 350 sccm, the deposition rate increases as the ratio of hexamethyldisilane (HMDS) to TEAB in the bubbler increased from 1/25 to 1/4 at a total precursor flow rate about 17 sccm as shown in figure 3.5. There exists a maximum deposition rate at the 1/4 ratio of HMDS/TEAB, after this point the deposition rate slightly decreases. It is worth to note that the films deposited at this ratio have a different composition as indicated in the IR spectroscopy of the films, indicating that the silicon additives were completely incorporated into the films. The membranes produced for the x-ray lithography mask characterized having the following properties: high x-ray and optical transmission, low tensile stress, free of hydrogen, and high mechanical strength.

3.3 IR Spectroscopy

The IR spectra of BN thin films deposited on silicon substrate show two typical absorption bands as in figure 3.6 after the effect of the substrate was removed using a blank substrate in the reference beam. A strong asymmetrical band centered at 1400 cm^{-1} is attributed to B-N stretching vibration and a sharper band at 800 cm^{-1} is attributed to B-N-B bending vibration (9-10,14,16-17,21-22,29-30,32,34-35,37-42). The broadness and frequency of the B-N stretching depends on the experimental conditions.

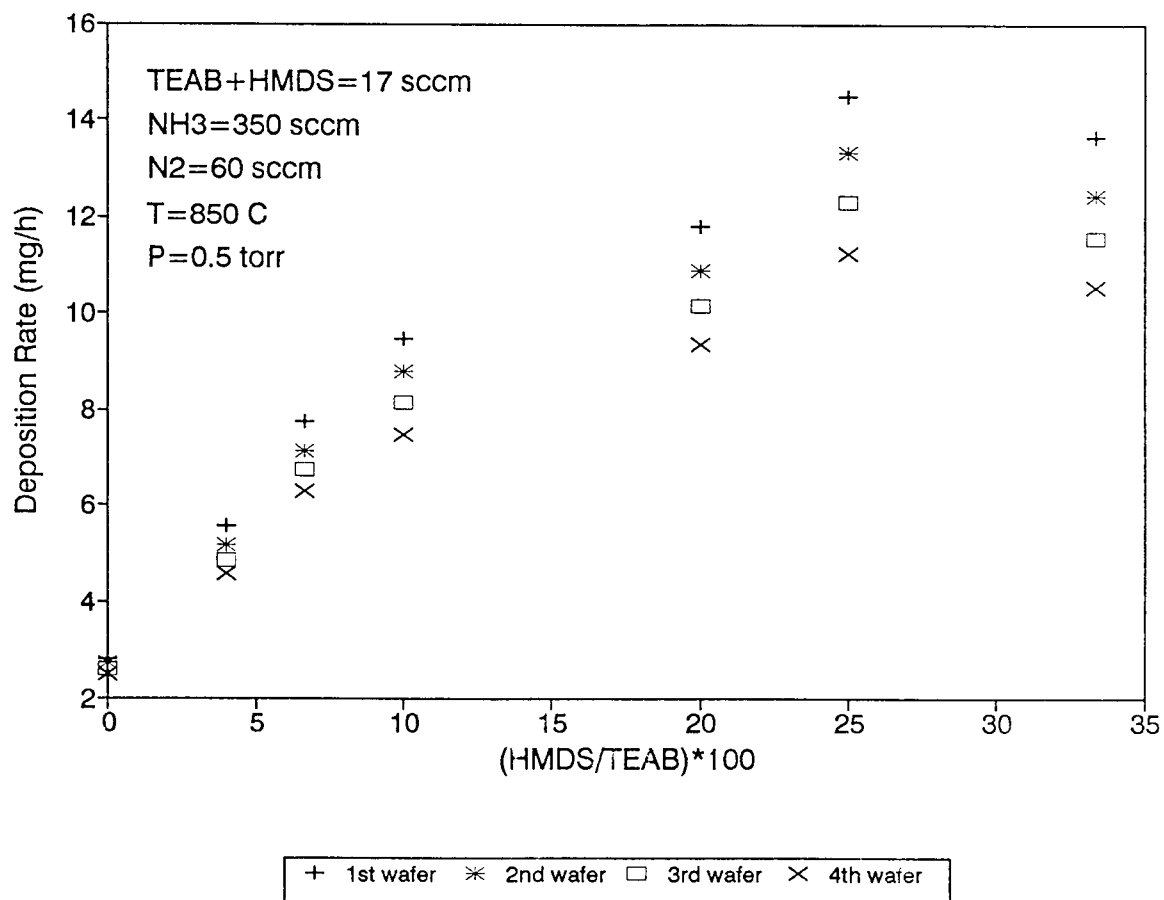


Figure 3.5 Effect of silicon additives on deposition rate for the reaction between NH_3 and liquid precursor mixture (HMDS and TEAB complex) at a constant temperature of 850°C and pressure of 0.5 torr.

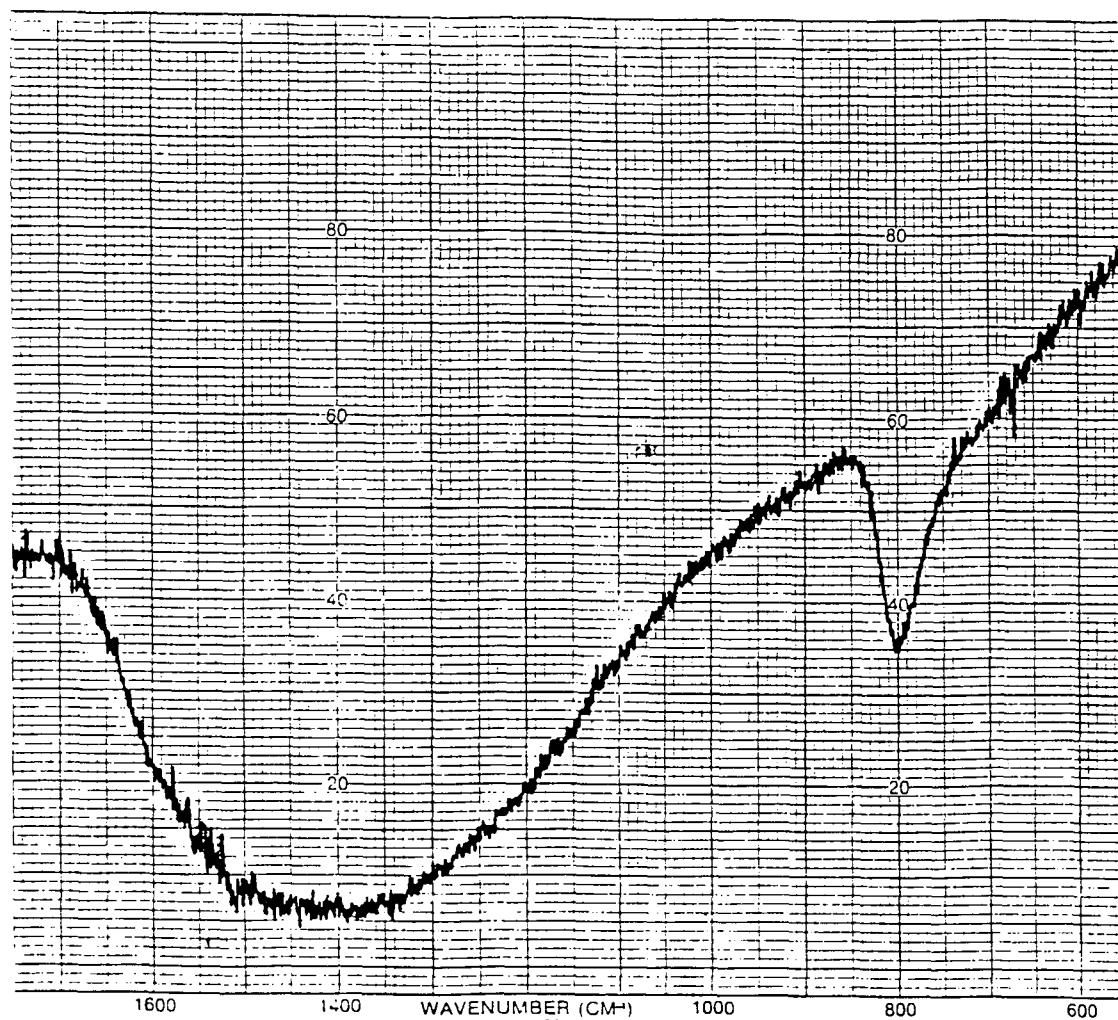


Figure 3.6 IR spectrum of typical BN films. Sample source was deposited at temperature of 850°C, pressure of 0.5 torr, TEAB flow rate of 17 sccm, and NH₃ flow rate of 350 sccm.

For the films deposited with no ammonia at constant conditions of pressure (0.5 torr) and TEAB flow (17 sccm), the IR spectrum exhibited a broad asymmetric B-N peak centered around 1250 cm^{-1} as well as a small B-H peak centered around 2560 cm^{-1} (10,21,32,34-35,37-40) at 600°C deposition temperature. At 650°C , the B-H peak disappeared while the B-N peak shifted to a higher wave number of 1300 cm^{-1} . The presence of a single peak remained until the deposition temperature increased to 750°C where an additional peak at 780 cm^{-1} due to the B-N-B out of plane vibration emerged. At 800°C and above, the IR spectrum flattened out indicating high signal absorption over the investigated range of 4000 to 200 cm^{-1} .

For films deposited with a constant NH_3/TEAB ratio of 10/1 and total pressure of 0.5 torr, the IR spectra for the deposition temperature range of 300 to 400°C exhibited absorption peaks close to 3400 cm^{-1} [(N-H) (32,35,39) or (O-H) (21,35,37,40,43)], 3220 cm^{-1} (N-H) (10,32,34-35,38,43), 2520 cm^{-1} (B-H), 1400 cm^{-1} , 900 cm^{-1} (Si-N,Si-H) (44), and 760 cm^{-1} (B-N-B). From 475 to 620°C , the 3220 cm^{-1} disappeared while the 1400 , 760 cm^{-1} shifted to 1350 , 790 cm^{-1} respectively. At 720°C , the peaks at 2520 , 900 cm^{-1} disappeared, while by 785°C only the 1400 and 800 cm^{-1} still remained reflecting the absence of any incorporated hydrogen. It is interesting to note that the amount of incorporated hydrogen, as determined by the IR peaks, is significantly lower in the case of films synthesized with no

ammonia indicating that most of the hydrogen in the films originates from the use of ammonia. Thus in the absence of ammonia, the films produced had an undetectable amount of hydrogen by IR at a significantly lower deposition temperature (650°C vs 785°C).

At constant conditions of temperature (850°C) and NH₃/TEAB ratio (10/1), no detectable change in the IR spectra was seen with changes in pressure over the range of 0.21 to 0.6 torr. At the constant deposition temperature of 850°C and pressure of 0.5 torr, the effect of varying the ammonia flow rate at a fixed TEAB complex flow rate of 17 sccm resulted in an increased IR transmission with the standard peaks appearing at 1400 and 800 cm⁻¹ for the lowest investigated flow rate of 80 sccm NH₃. A further increase in NH₃ flow rate resulted in no detectable change in the IR spectra.

At the constant deposition temperature of 850°C, total pressure of 0.5 torr, 350 sccm NH₃ flow, and 17 sccm total precursor flow with additional silicon additives to the TEAB complex resulted in an IR spectra with two strong absorption peaks at 1300 cm⁻¹, B-N stretching, and 950 cm⁻¹, suggested to be Si-N stretching, as showed in figure 3.7. The IR spectra indicated the film composition was strongly influenced by the incorporated silicon. In the range of HMDS/TEAB ratio from 1/25 to 1/5, unsaturated silicon reflected two weak absorptions at 2180 cm⁻¹ (Si-H) (44), and 620 cm⁻¹ (Si) (17,22,37), while an undetermined additional

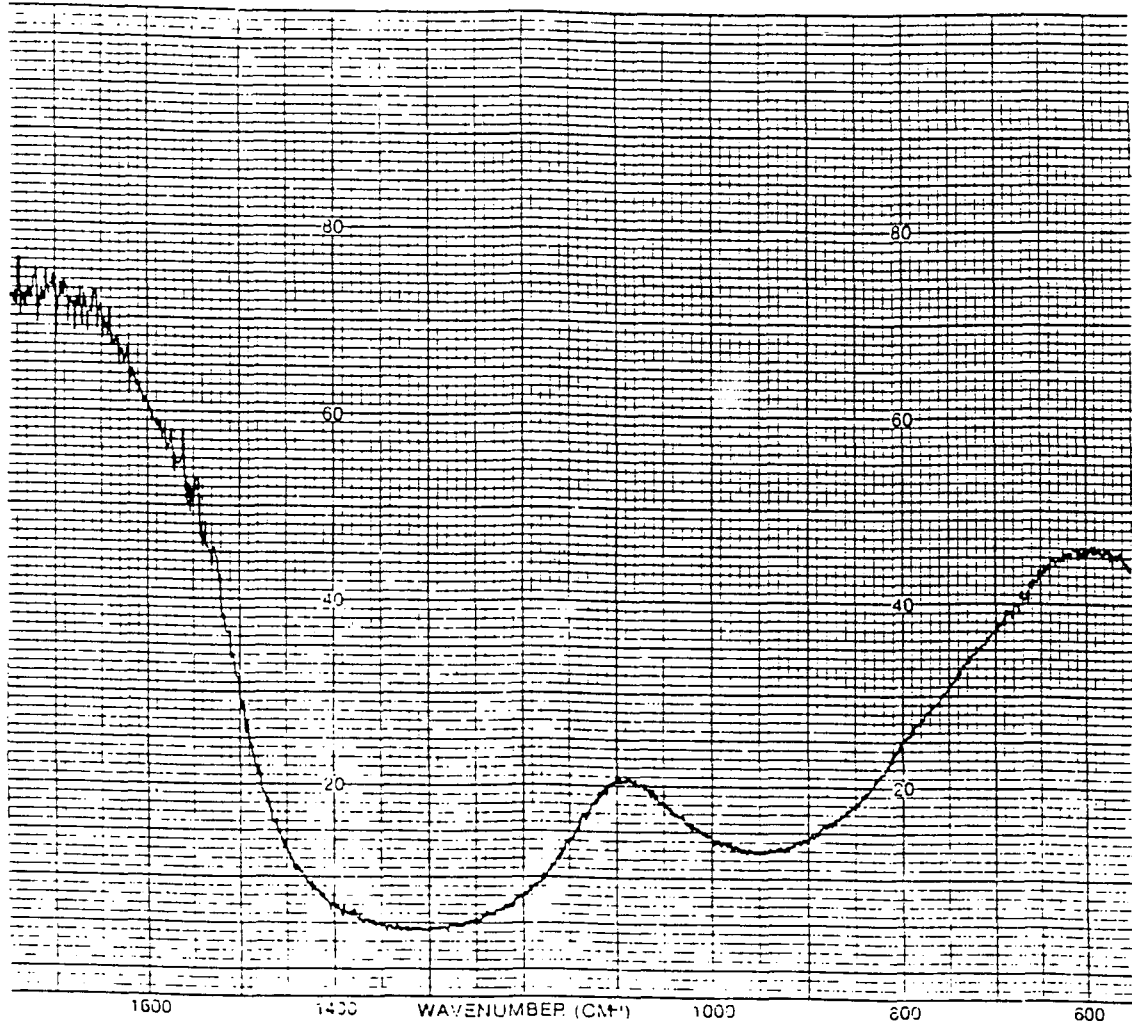


Figure 3.7 IR spectrum for BN films incorporated with silicon. Sample source deposited at temperature of 850°C, pressure of 0.5 torr, NH₃ flow rate of 350 sccm, and HMDS/TEAB ratio of 1/4.

peak formed at 970 cm^{-1} . As the ratio increased to 1/4, the peaks centered at 2180 , 620 cm^{-1} disappeared and the 970 , 790 cm^{-1} peaks merged into a single broad peak at 950 cm^{-1} . All cases a relatively weak N-H (or O-H) absorption around 3420 cm^{-1} was present.

3.4 Refractive Index

The refractive index of BN films is strongly dependent on the experimental conditions varying from 1.7 to 2.5. For a constant deposition pressure of 0.5 torr and NH_3/TEAB ratio of 10, the refractive index depends on temperature is shown in figure 3.8. There exists a refractive index about 2.1 near 400°C and decreases to 1.8 with increasing temperature at 550°C then increases with further increased temperature. It is interesting to note that this curve is generally consistent to the deposition rate curve as plotted in figure 3.2 and in agreement with Capio's study (25). As shown in figure 3.9, the refractive index decreases with increasing ammonia flow rate in a simple manner.

Incorporated silicon sharply increases the refractive index from 1.7 to about 2.1 with a constant deposition temperature of 850°C , pressure of 0.5 torr, and ammonia flow rate of 350 sccm as shown in figure 3.10. This constant value of 2.1 indicates that the film composition is relatively constant at around 1/4 ratio of HMDS/TEAB and the increased value of the refractive index is also reflected in a slightly decrease in the optical transmission.

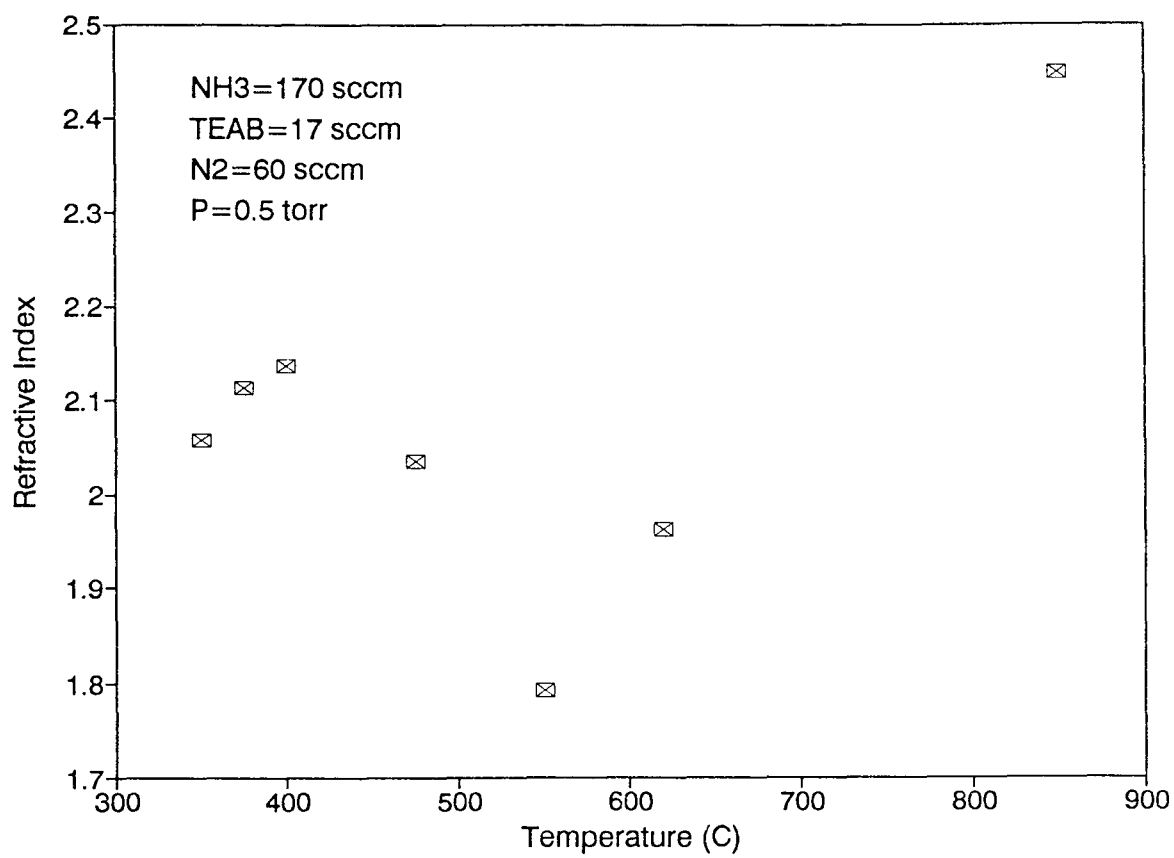


Figure 3.8 Effect of temperature on refractive index for films deposited at constant pressure and flow rate.

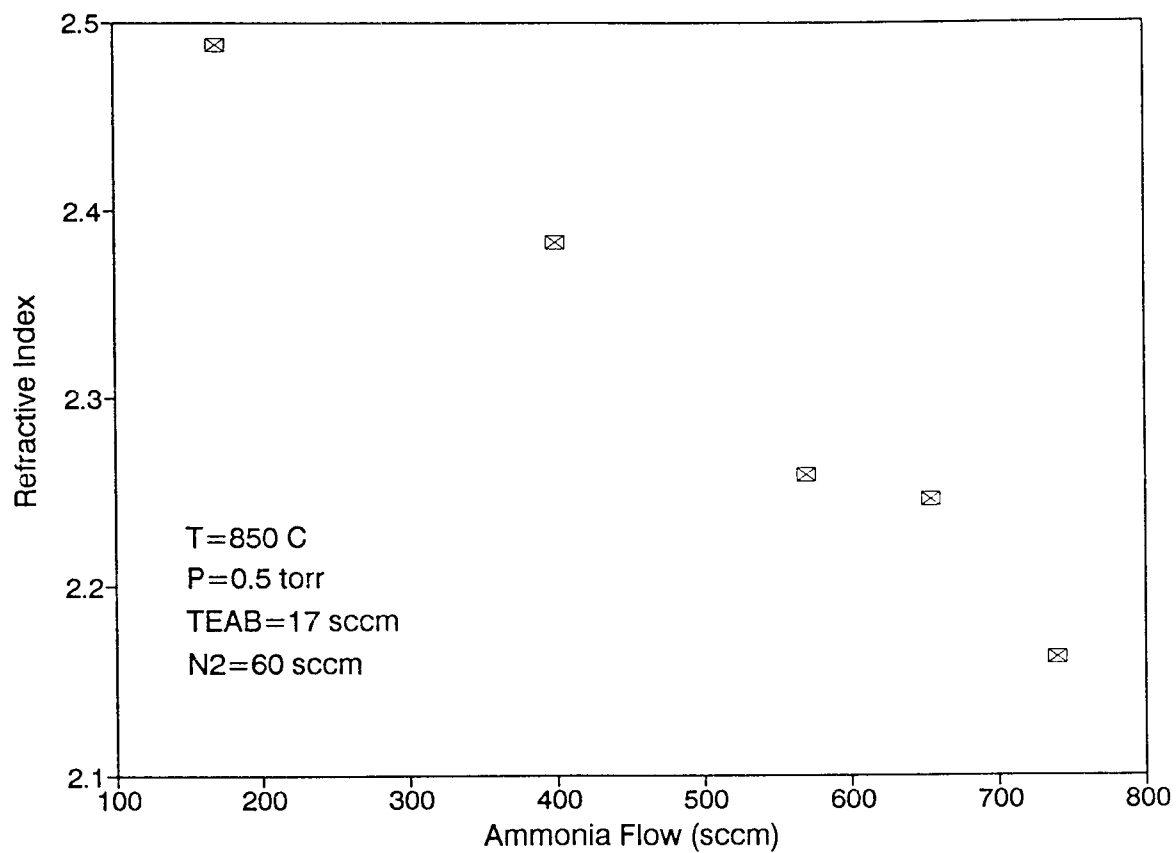


Figure 3.9 Effect of ammonia flow rate on refractive index for films deposited at constant temperature, pressure, and TEAB flow rate.

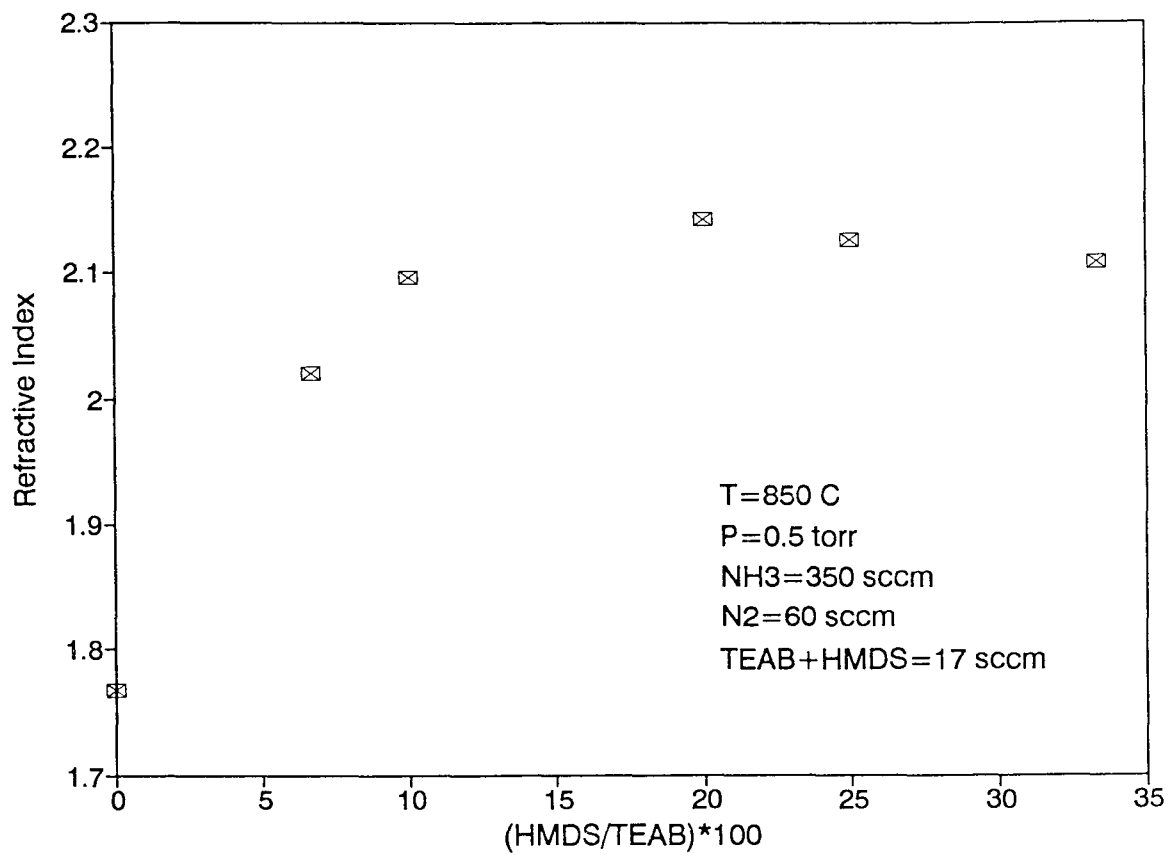


Figure 3.10 Effect of silicon additives on refractive index for films deposited at constant temperature, pressure, and ammonia flow rate.

3.5 Density

The density, D , of the film was calculated from the film thickness, the film weight, and the wafer surface area using the following formula:

$$D = \frac{\Delta W}{A \times T}$$

where ΔW is the film weight, A is the wafer surface area, and T is the film thickness measured by nanospectrometer. The density of the boron nitride films was found to vary between 1.5 and 2.5 g/cm³.

For a constant deposition temperature of 850°C and pressure of 0.5 torr, the density of films only slightly change with increased ammonia flow at around 2.2 g/cm³ as shown in figure 3.11. This constant value indicates a stoichiometric BN film formed by the saturated reactant gaseous due to the diluted precursor complex by addition of ammonia.

Incorporation of silicon into the boron nitride strongly increase the film density as shown in figure 3.12. There exists a maximum value of 2.52 at 1/4 ratio of HMDS/TEAB in accordance with the previous deposition rate study (refer to figure 3.5).

3.6 Optical Transmission Spectroscopy

The optical transmission of the boron nitride thin films deposited on fused quartz substrates has been measured in the ultraviolet-visible region (200-800 nm wavelength) and

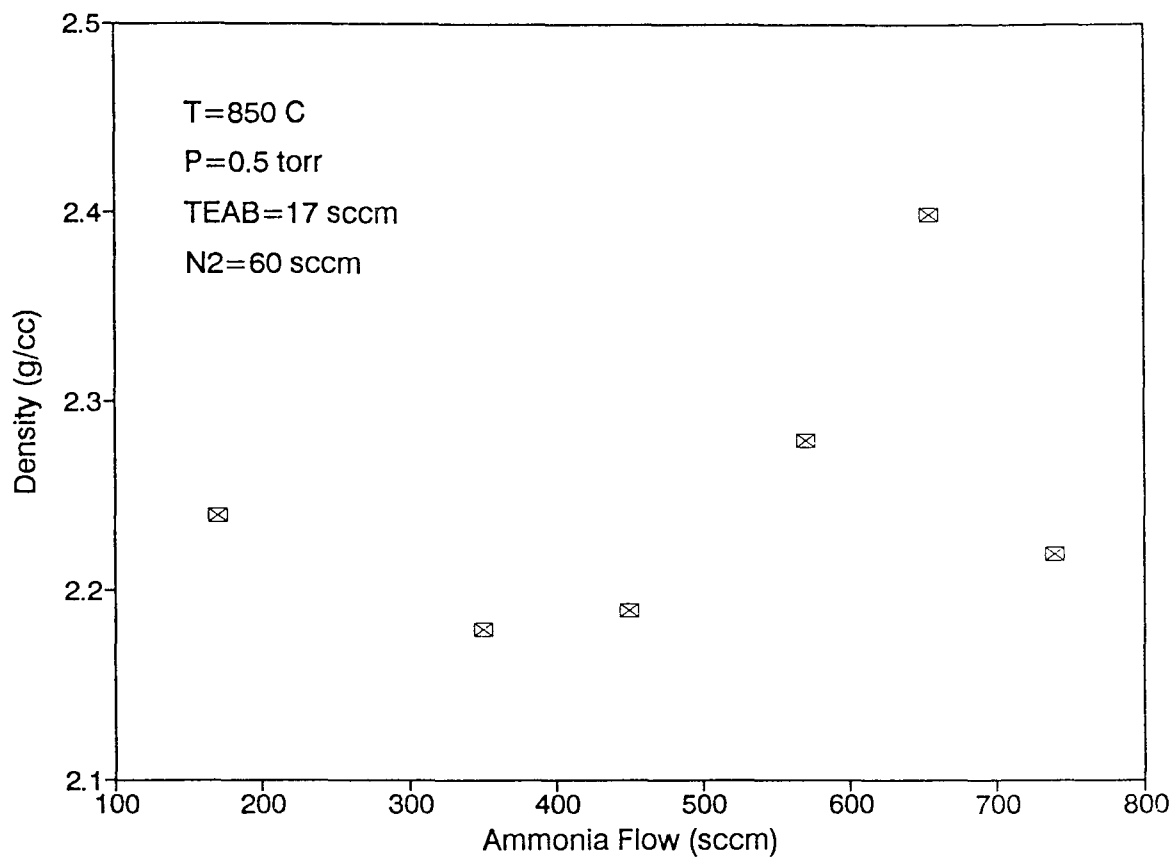


Figure 3.11 Effect of ammonia flow rate on the density of the films.

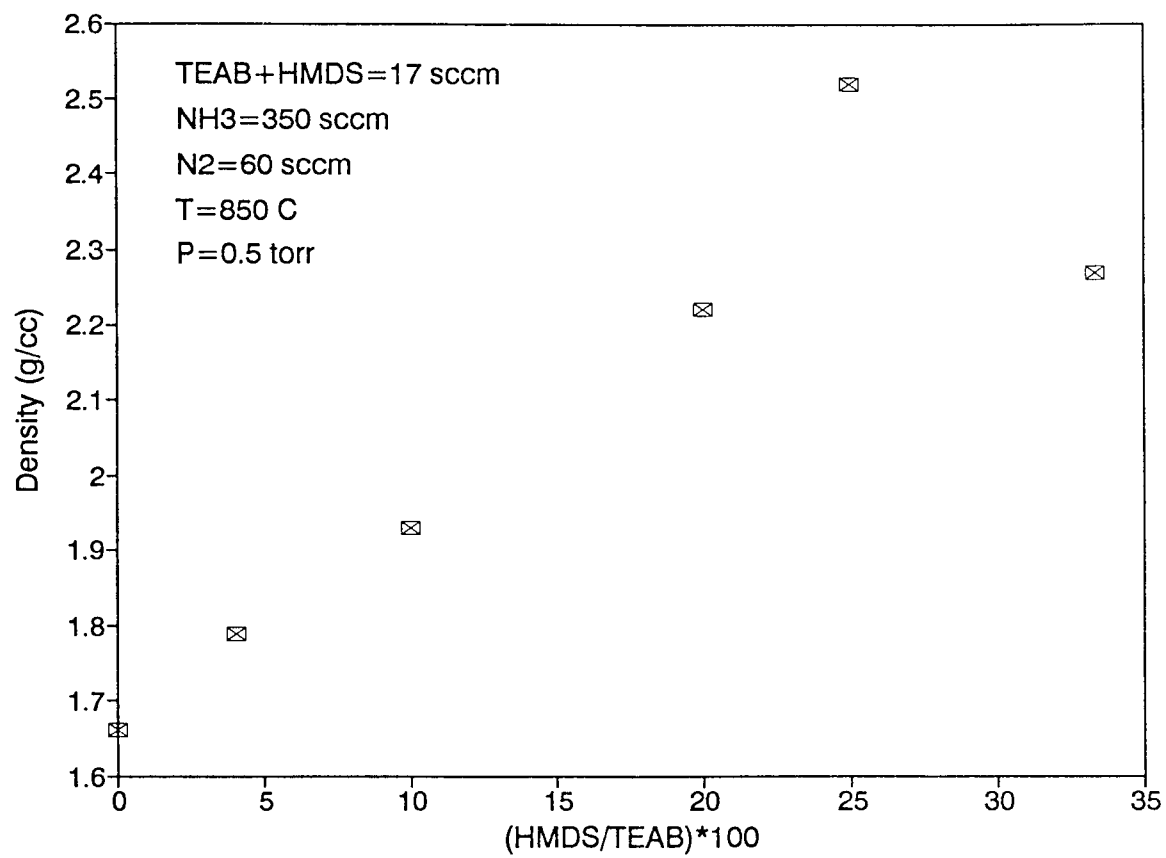


Figure 3.12 Effect of silicon additives on the density of the films.

the absorption coefficients have been calculated for a wavelength of 633 nm which was considered to represent the absorption in the visible region (35). As shown in figure 3.13, the optical transmission was determined by the midpoint of the schematically maximum and minimum transmission curve at 633 nm wavelength. The absorption coefficient, α , was calculated using the equation $I = I_0 \exp(-\alpha T)$; where I is the radiation intensity and T is the film thickness. By determining the optical transmission I/I_0 , then calculating the thickness by the film weight and the pre-calculated film density on the silicon sample from the same run, thereby the absorption coefficient can be carried out.

For films deposited with no ammonia were observed to be dark in all cases and 0% optical transmissions were measured suggesting the presence of a carbon-boron-rich composition. With addition of ammonia (10/1 to TEAB), highly transparent (>70%) films, about one micron thickness, were deposited at the temperature below 620°C. As the temperature higher than 720°C, all deposits become dark reflecting the changing in reaction mechanisms.

Pressure was found to be the smallest factor on the optical property. In the pressure range from 0.21 to 0.6 torr, all deposits were found to be dark at a fixed temperature of 850°C and NH_3/TEAB ratio of 10/1.

For a constant temperature of 850°C, total pressure of 0.5 torr, and TEAB flow rate of 17 sccm, increasing the

Trace A Operator W. Sample E244
 Mode IT SSM (nm) 2.0 Smoothing (sec) 0.2
 Ord Max/Min 100.0 0.0 ML Max/Min (nm) 900.0 200.0
 Speed (nm/min) 100
 # Peaks, threshold 1.0
 Min 784.6 nm, 79.1 Min 749.9 nm, 81.1
 Max 685.2 nm, 91.7 Max 669.2 nm, 90.9
 Min 598.6 nm, 78.5 Max 543.2 nm, 87.0
 Min 486.7 nm, 39.2 Max 457.2 nm, 66.0

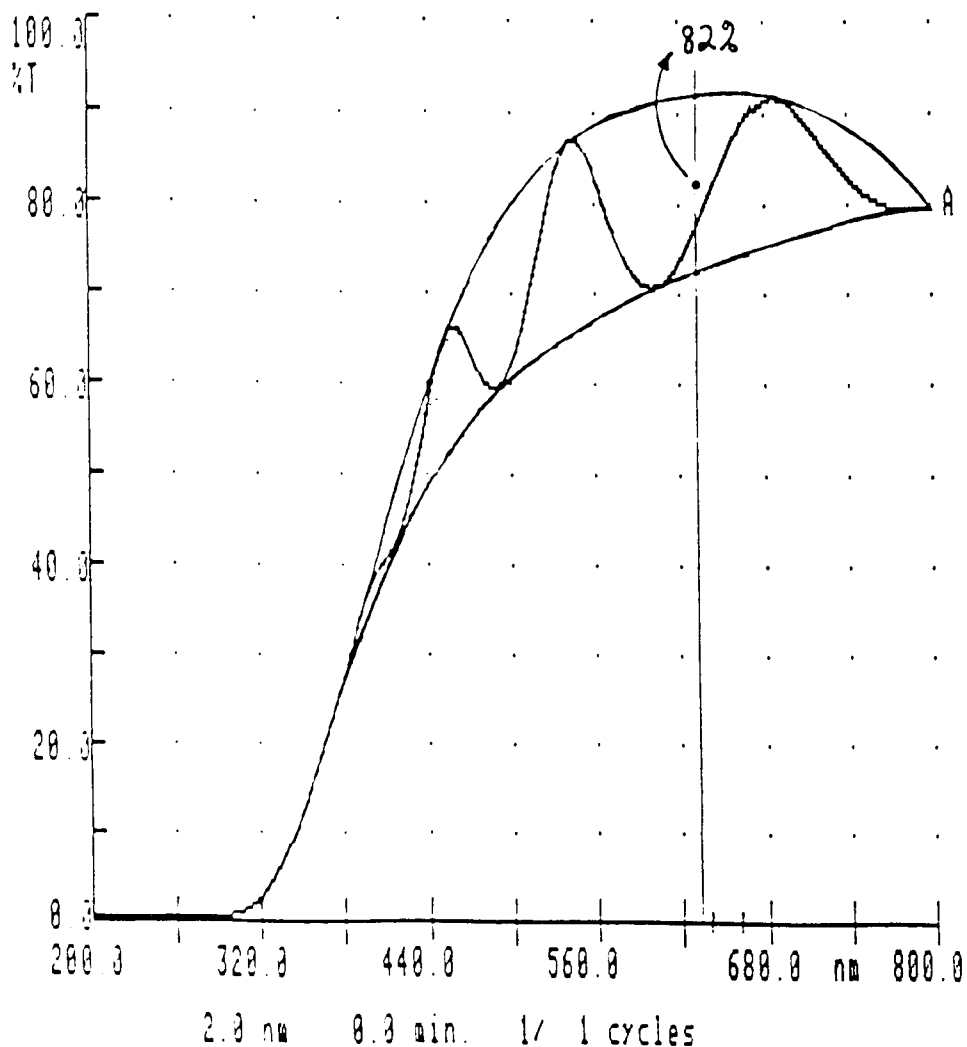


Figure 3.13 Determination of optical transmission of the films. Sample source deposited at temperature of 475°C, pressure of 0.5 torr, TEAB flow rate of 17 sccm, and ammonia flow rate of 170 sccm.

ammonia flow rate will result in an improve in the optical transmission, i.e. reducing the absorption coefficient, as shown in figure 3.14.

With incorporated of silicon into the film only a slightly decreases the film transmission was observed and the absorption coefficients shift between 0.4 and 0.8 ($10^4/\text{cm}$) as shown in figure 3.15.

3.7 Stress

The temperature dependence of the film stress was seen to be compressive above 700°C and tensile below that temperature as seen in table 3.1 and 3.2. Without ammonia, the films deposited at 600°C were seen to be highly tensile and revealed severe cracking on the surface. By association of ammonia into the complex precursor (10/1 ratio of NH_3/TEAB), the increased nitrogen content reduced the tensile level in the temperature range from 350 to 475°C and the films did not show visible cracking. For the temperature below 325°C and above 550°C , the films were compressive. The tensile nature of these films is believed to be due to the presence of incorporated hydrogen.

In addition of ammonia flow to the precursor at a constant temperature of 850°C and a total pressure of 0.5 torr, the stoichiometric hydrogen-free films deposited on silicon were compressive in nature (Table 3.3) and thus not suitable for preparation of membranes used as x-ray mask substrates.

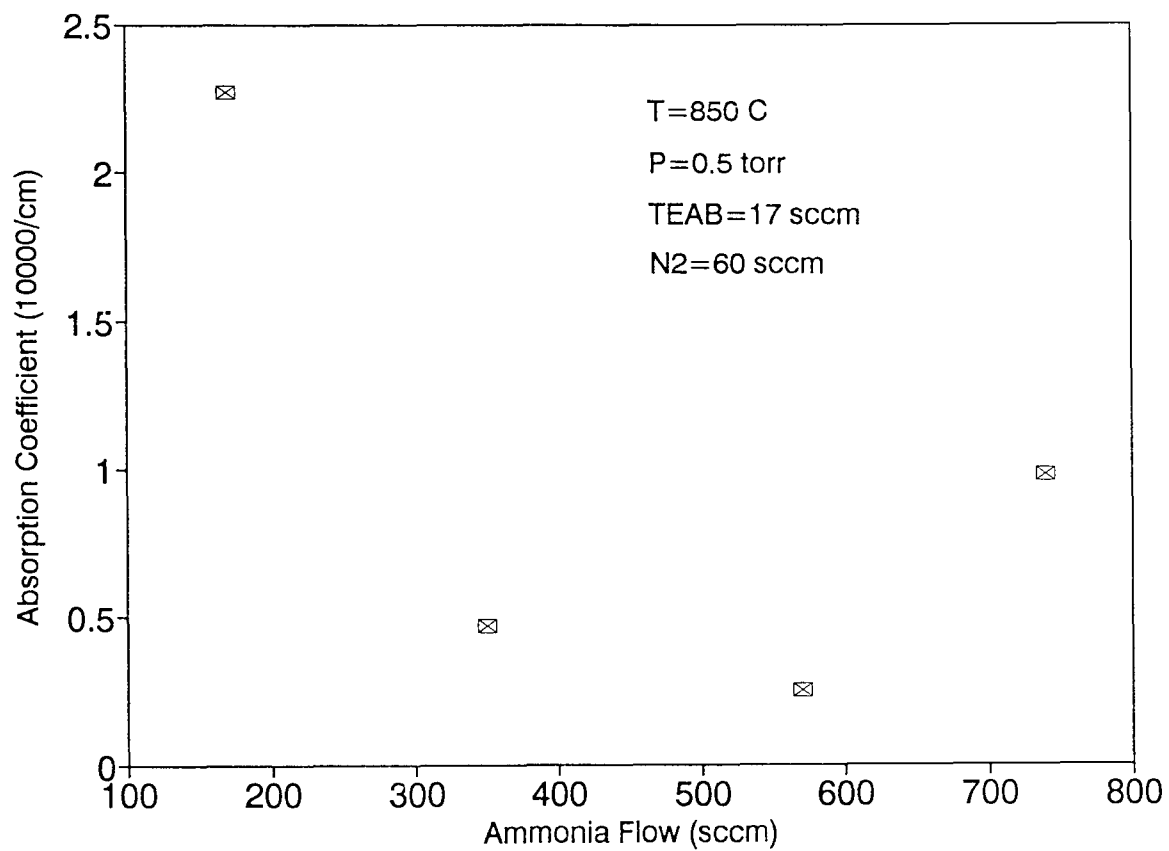


Figure 3.14 Effect of ammonia flow rate on the absorption coefficient of the films.

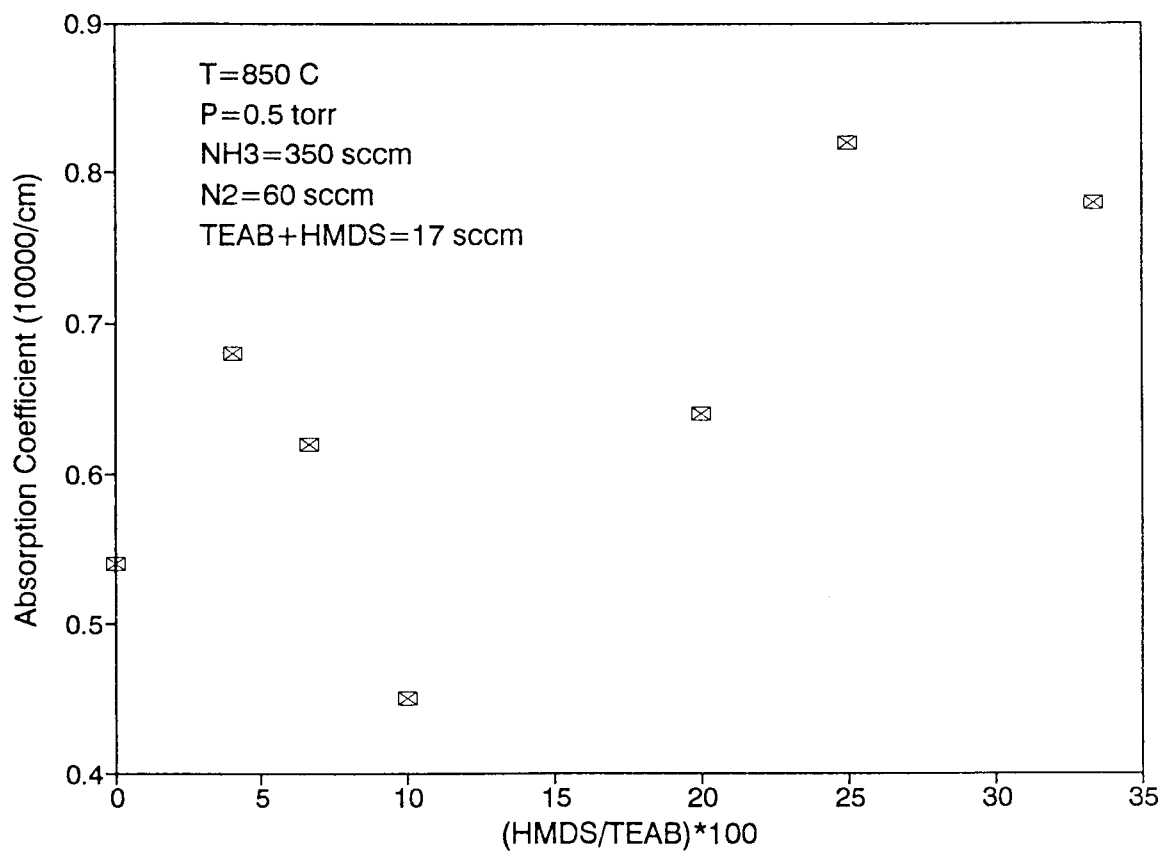


Figure 3.15 Effect of silicon additives on the absorption coefficient of the films.

Table 3.1 Effect of temperature on stress for films deposited with no ammonia (P=0.5 torr, TEAB=17 sccm, N₂=60 sccm).

Sample I.D.	Temperature (°C)	Thickness (Å)	Stress (MPa)
64	600	7500	670
74	650	6900	230
69	700	6100	- 50
71	750	7100	-270
72	800	8000	-220
73	850	6800	-200

Table 3.2 Effect of temperature on stress for films deposited with ammonia present (P=0.5 torr, NH₃=170 sccm, TEAB=17 sccm, N₂=60 sccm).

Sample I.D.	Temperature (°C)	Thickness (Å)	Stress (MPa)
53	300	2700	-180
32	325	6200	-110
23	350	8900	70
25	375	10500	90
34	400	14900	90
35	475	4100	110
13	550	27312	90
31	550	4600	- 50
36	785	5700	- 70
57	850	4900	-220

Table 3.3

Effect of NH₃ flow rate on stress (T=850°C, P=0.5 torr, TEAB=17 sccm, N₂=60 sccm).

I.D.	NH ₃ Flow (sccm)	Thick. (Å)	Stress (MPa)
73	0	6800	-200
15	80	5800	-170
57	170	4900	-220
41	350	7500	- 90
67	400	4800	-130
68	450	5900	- 80
43	570	9900	- 40
70	655	4300	-120
66	740	8200	- 90

Table 3.4

Effect of silicon additives on stress (T=850°C, P=0.5 torr, NH₃=350 sccm, N₂=60 sccm).

I.D.	HMDS/TEAB	Thick. (Å)	Stress (MPa)
97	0	6100	- 60
77	1/25	11600	-250
101	1/15	9300	-210
112	1/10	5000	- 80
103	1/5	10900	- 10
E716	1/4.5	10000	200
115	1/4	6600	130
113	1/3	5500	160

Table 3.5 Effect of deposition pressure on stress

(T=850°C, TEAB=17 sccm, NH₃=170 sccm, N₂=60 sccm).

Sample I.D.	Pressure (torr)	Thickness (Å)	Stress (MPa)
50	0.21	10500	-240
52	0.3	5500	-200
54	0.4	4700	-130
57	0.5	4900	-220
56	0.6	6300	-200

The effects of incorporating silicon into the stoichiometric boron nitride films not only enhanced the mechanical strength, but also rendered such films tensile. As shown in table 3.4, the stress value increased as the HMDS/TEAB ratio increased. By this successful incorporation of silicon into the BN films, a desired film stress level can be accurately controlled. Pressure shows almost no influence on stress as seen on table 3.5. The stress of films is not only a function of experimental variables but also a strong function of film thickness, that is why the data is not plotted.

3.8 Mechanical Properties

The hardness and Young's modulus of the boron nitride films were measured with a nanoindenter. Figure 3.16, 3.17, 3.18 and 3.19 represent plots of hardness and Young's modulus as a function of temperature for films produced without and with ammonia. In both cases, there appears to be a decrease in both values as the deposition temperature is raised up to 850°C. One thing worth to note is that most films deposited at high temperature were also chemically unstable as found to change in surface color after a long time storage in the envelop. The hardness and Young's modulus as a function of pressure are shown in figure 3.20 and 3.21.

For constant conditions of temperature (850°C) and pressure (0.5 torr), the increase in ammonia flow rate has the effect of decreasing both the hardness and Young's

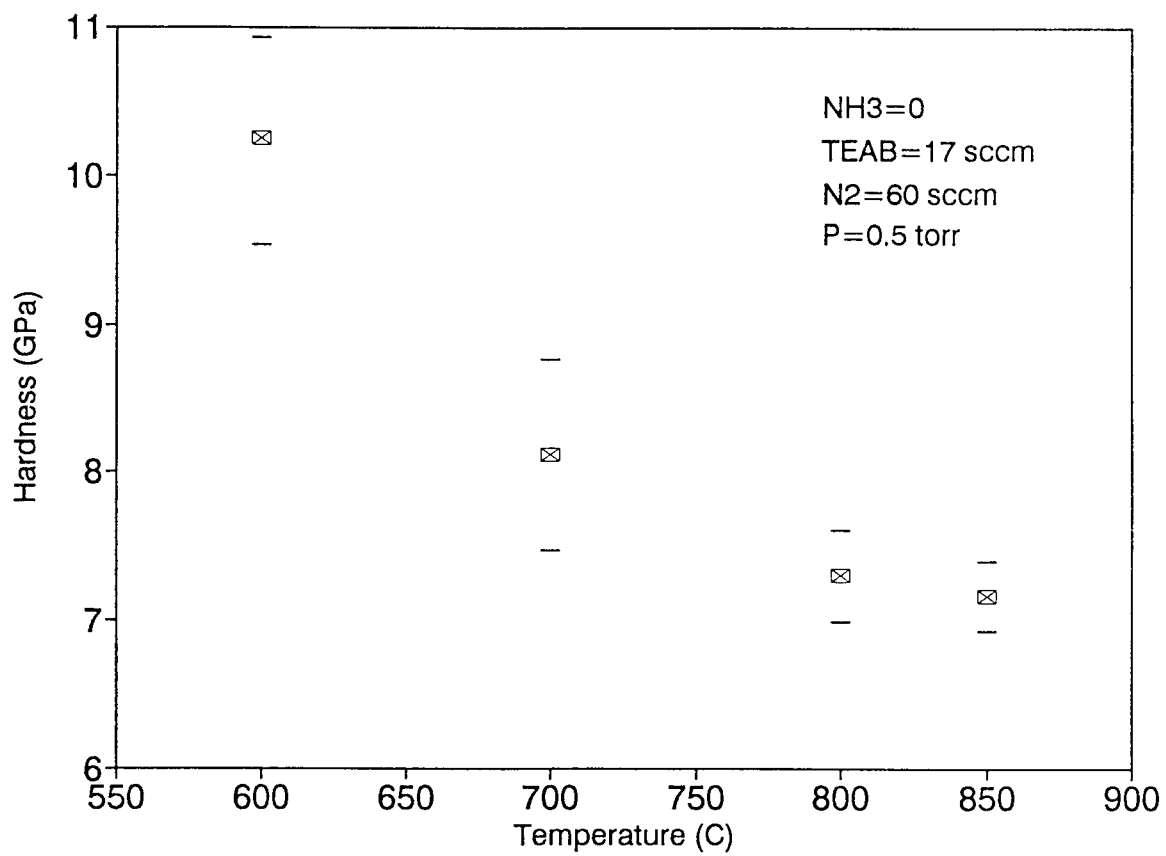


Figure 3.16 Effect of temperature on hardness of BN films prepared without the use of ammonia.

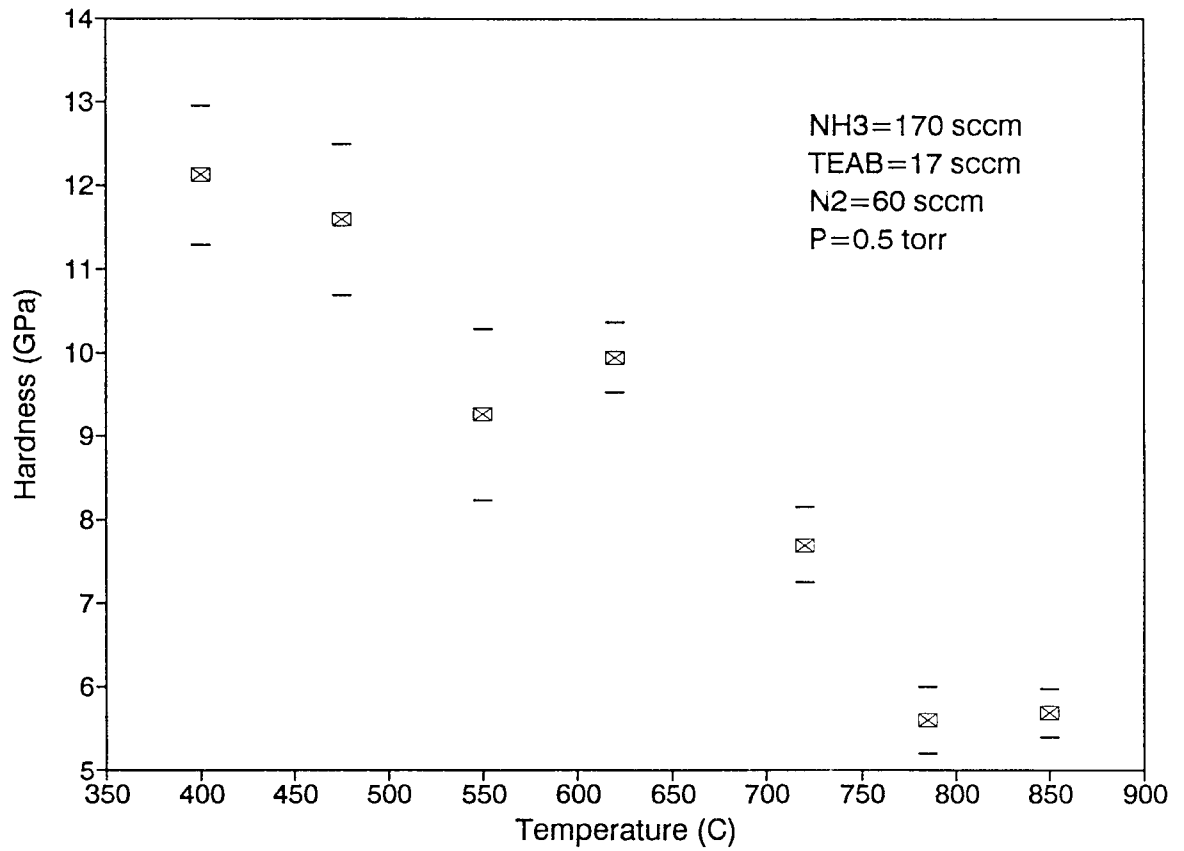


Figure 3.17 Effect of temperature on hardness of BN films prepared using ammonia.

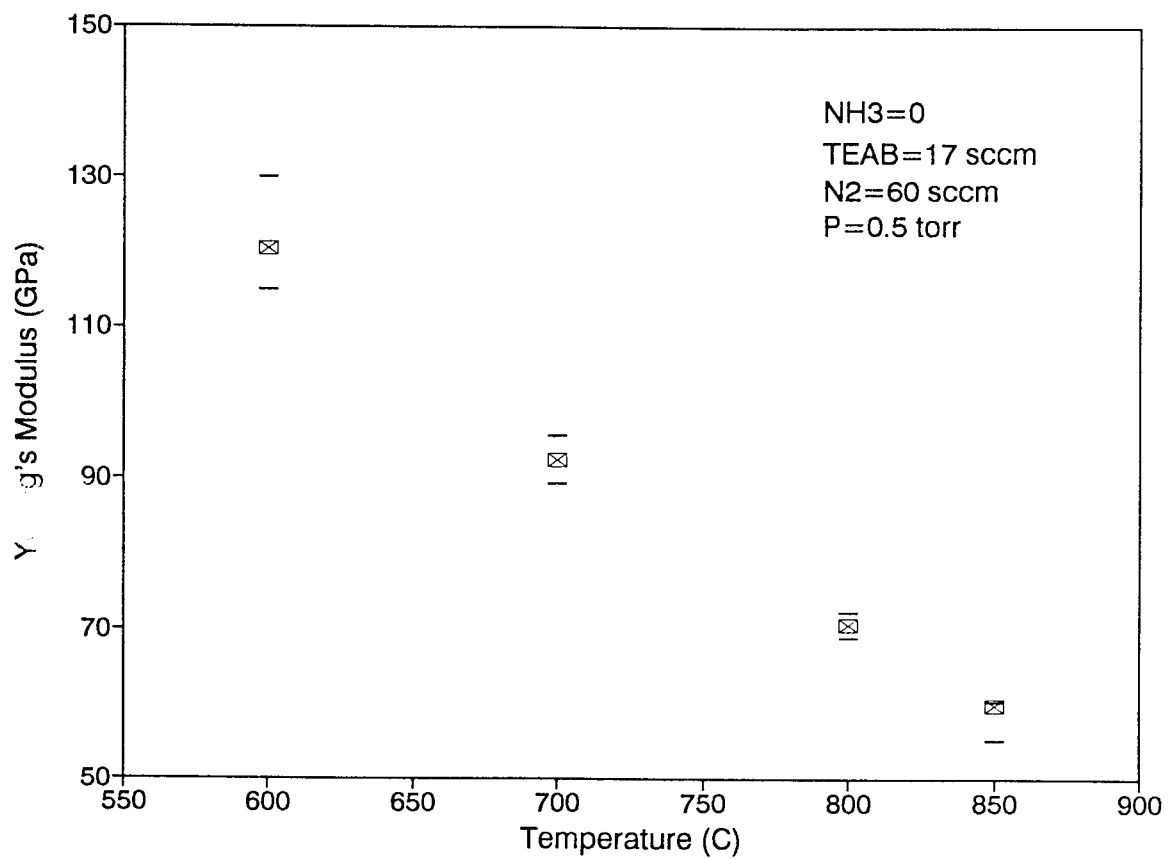


Figure 3.18 Effect of temperature on Young's modulus of BN films prepared without the use of ammonia.

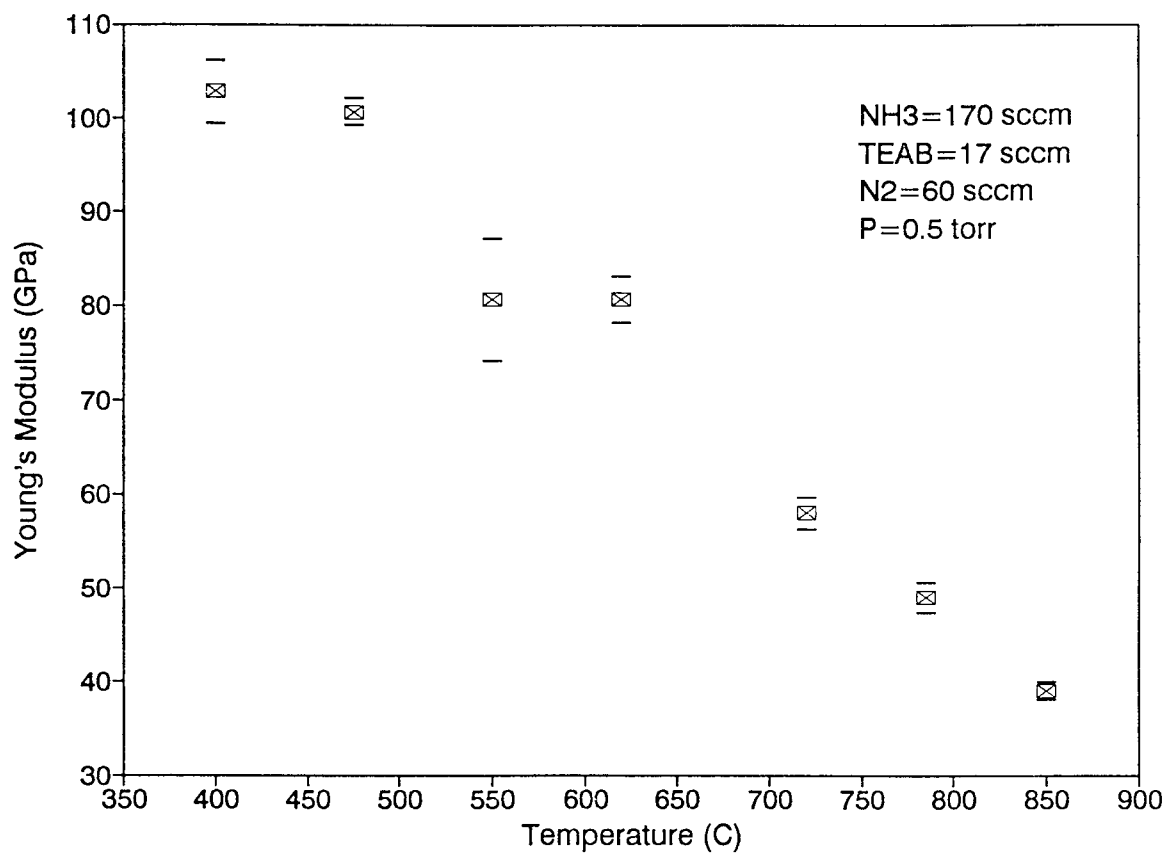


Figure 3.19 Effect of temperature on Young's modulus of BN films prepared using ammonia.

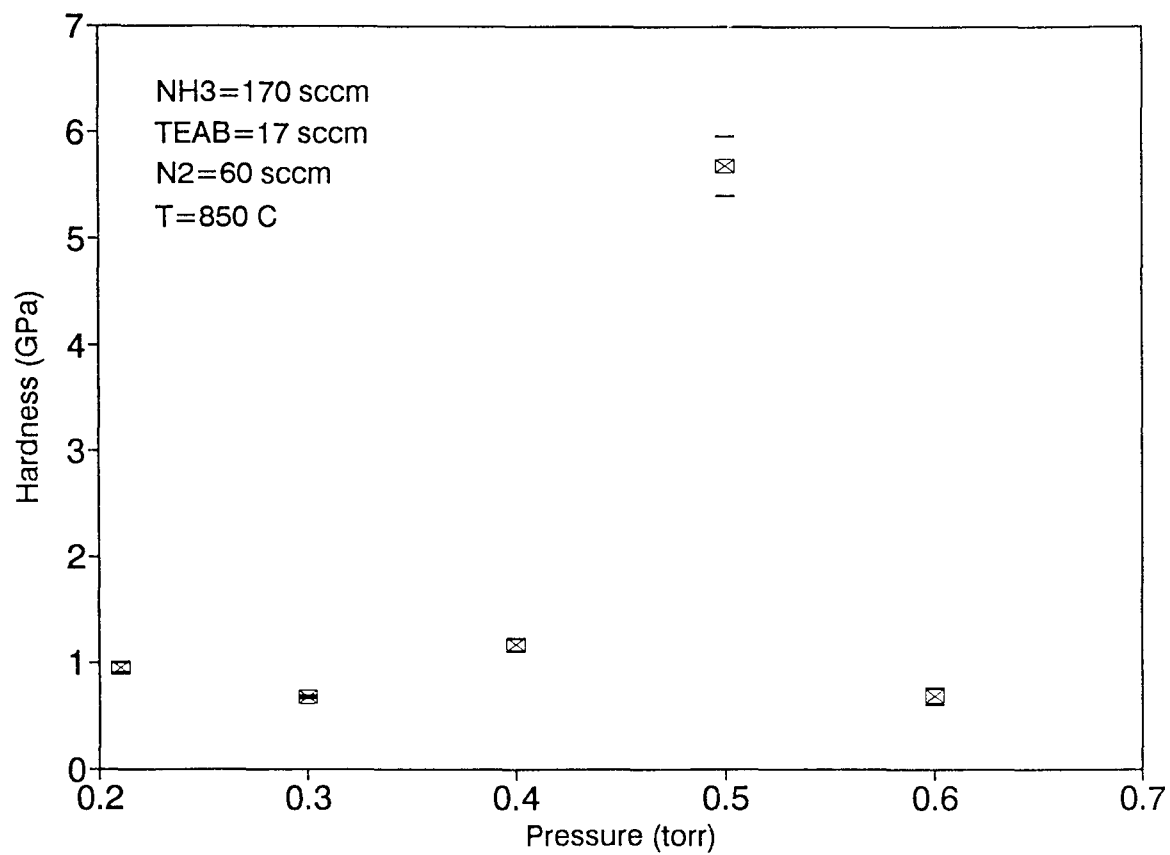


Figure 3.20 Effect of pressure on hardness for films deposited at constant temperature and flow rate.

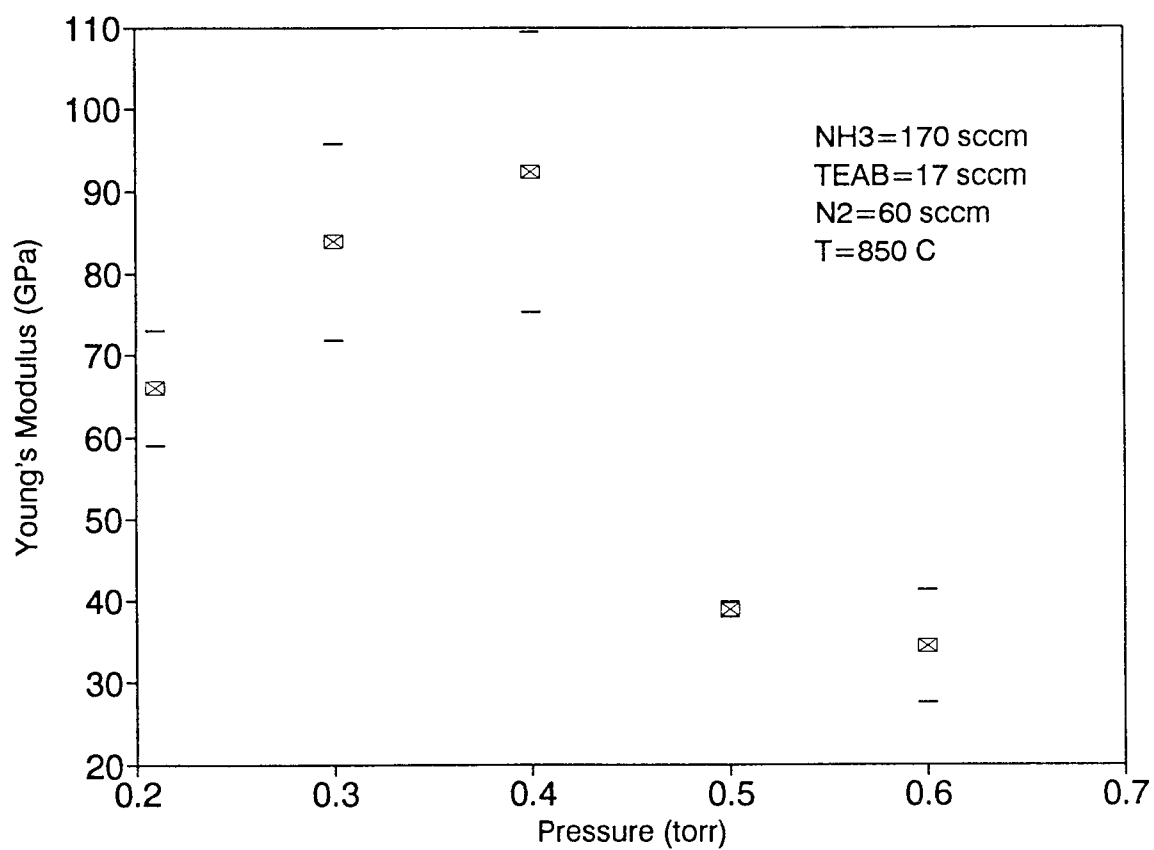


Figure 3.21 Effect of pressure on Young's modulus for films deposited at constant temperature and flow rate.

modulus as seen in figure 3.22 and 3.23. This mirrors the ability of the films to form membranes as the NH_3 flow rates increase to 350 sccm. Above this flow rate, the films were observed to disintegrate readily in the KOH etch.

Incorporation of silicon into the boron nitride films at a fixed temperature of 850°C , pressure of 0.5 torr, and NH_3 flow rate of 350 sccm strongly enhance the hardness and Young's modulus of films as plotted in figure 3.24 and 3.25 respectively. This enhancement in mechanical properties of the films in turn results in a much higher durability in an etching solution, e.g. KOH, making it possible to prepare a membrane.

3.9 Annealing Effect

Films deposited at 475°C , 0.5 torr with a constant NH_3/TEAB ratio of 10/1 were highly optically transparent, highly mechanically strong, and slightly tensile in stress, but hydrogen was incorporated into the film at this relatively low temperature as detected in the IR spectrum. This hydrogenated boron nitride will cause the films to be unsuitable as x-ray lithography mask materials due to the radiation damage effect (32-34). Annealing such films up to 1050°C showed that the process apparently affects the film properties. As shown in figure 3.26, the IR spectrum indicates the hydrogen absolutely removed while the mechanical hardness and modulus remain stable as shown in figure 3.27.

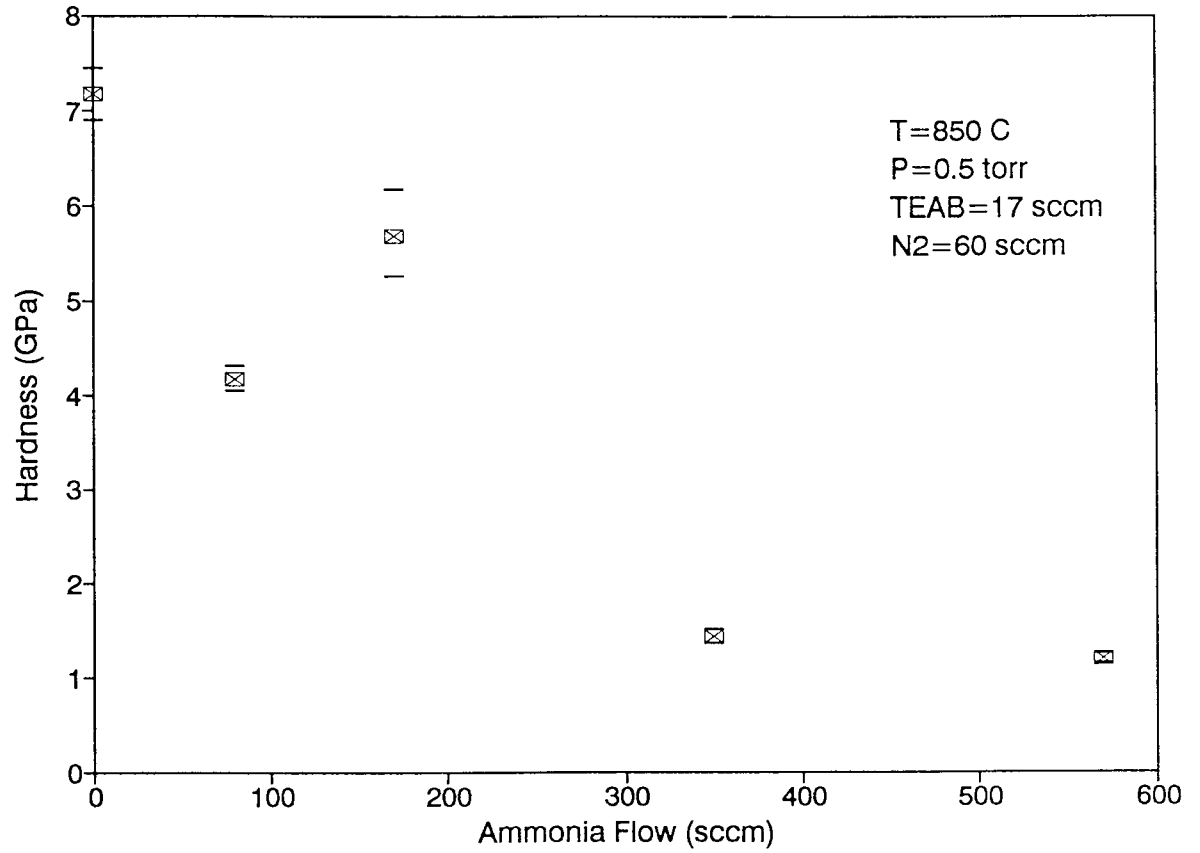


Figure 3.22 Effect of ammonia flow rate on hardness for films deposited at constant temperature, pressure, and TEAB flow rate.

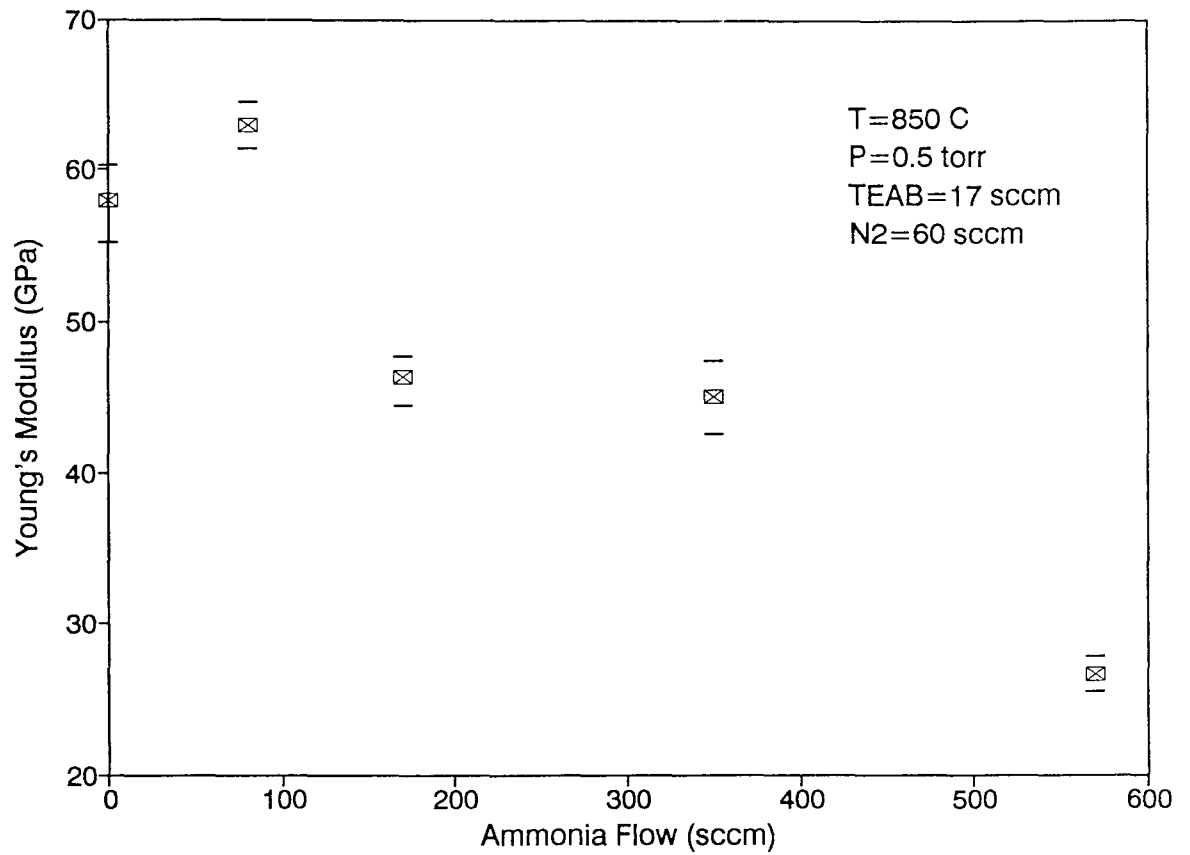


Figure 3.23 Effect of ammonia flow rate on Young's modulus for films deposited at constant temperature, pressure, and TEAB flow rate.

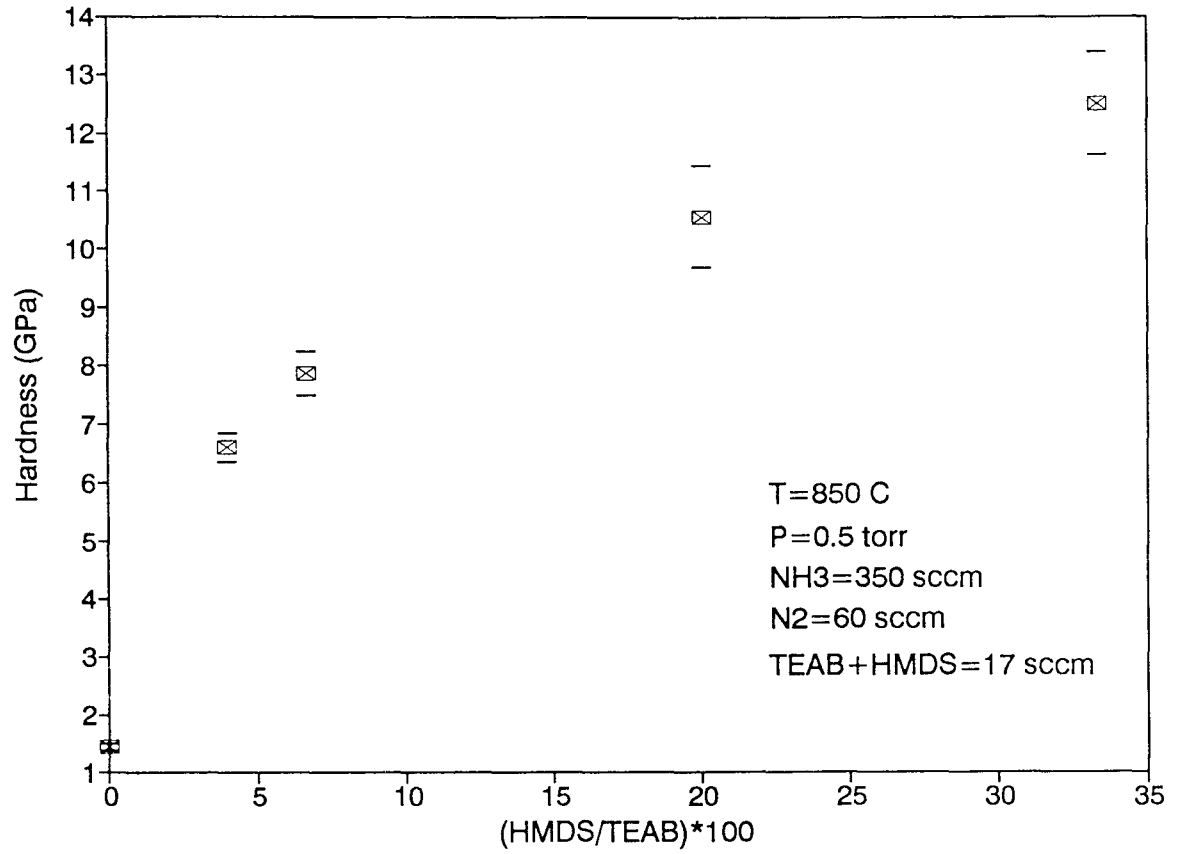


Figure 3.24 Effect of silicon additives on hardness for films deposited at constant temperature, pressure, and ammonia flow rate.

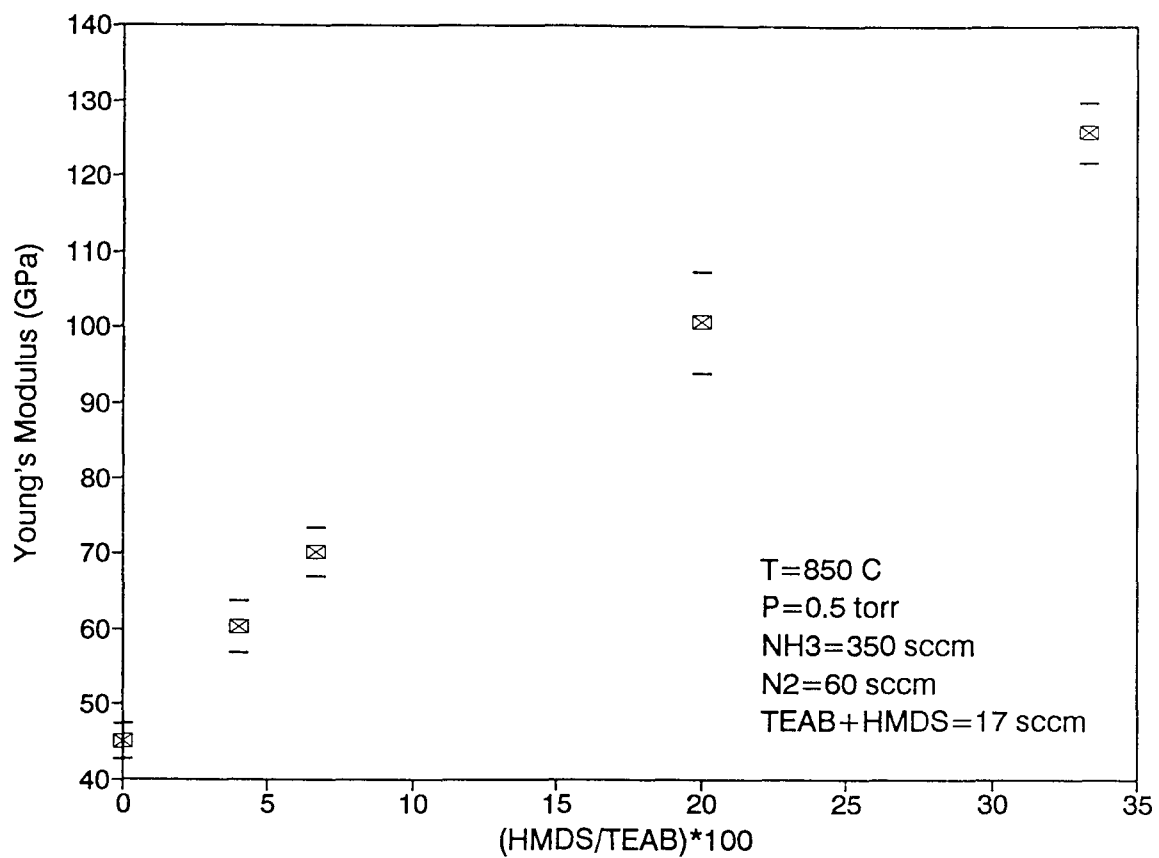


Figure 3.25 Effect of silicon additives on Young's modulus for films deposited at constant temperature, pressure, and ammonia flow rate.

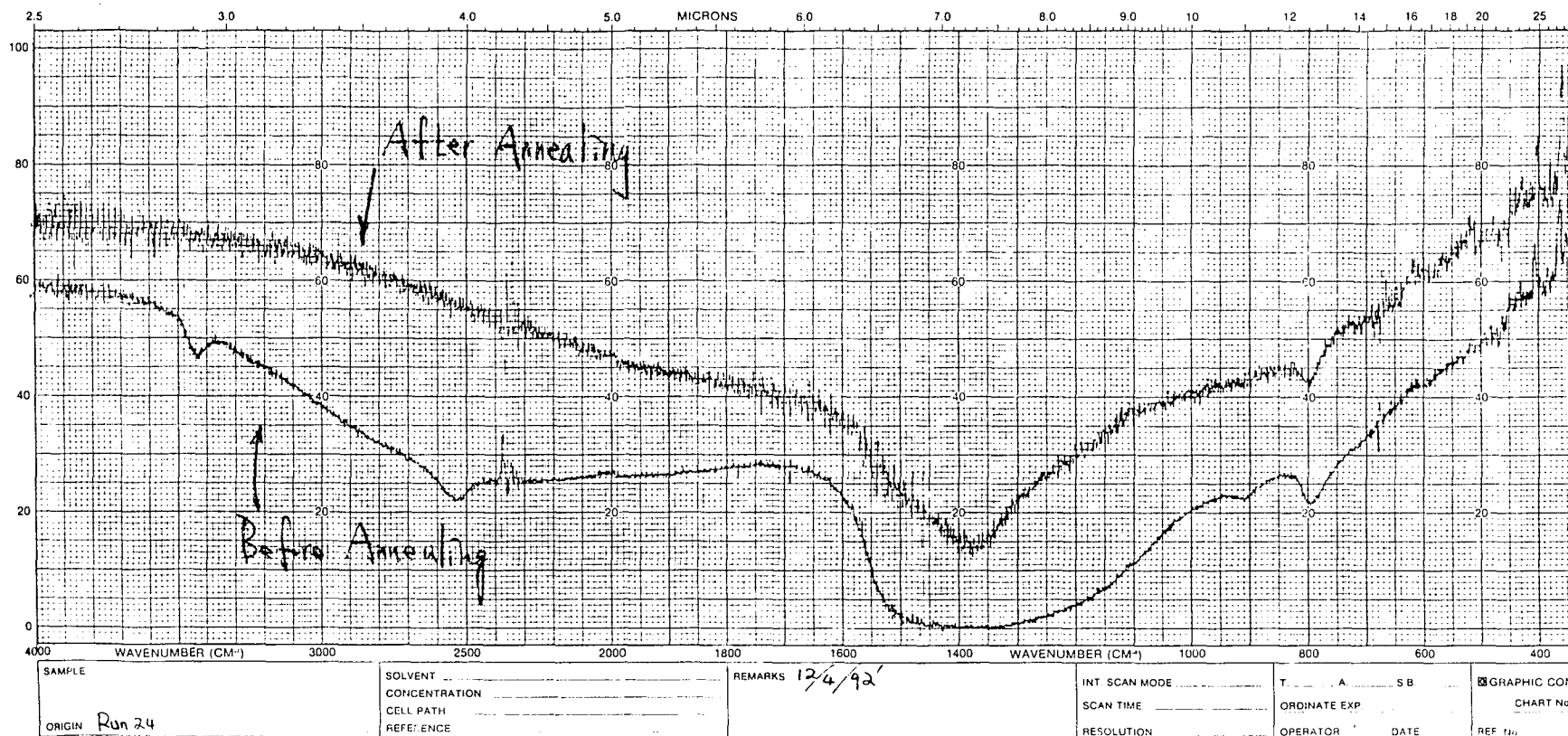


Figure 3.26 Annealing effect on the IR spectra for the films deposited at 475°C and annealed to 1050°C. The higher spectrum is for film annealed to 1050°C. After annealing, the 3420 cm⁻¹ (N-H) and 2520 cm⁻¹ (B-H) absorption peaks were almost disappear.

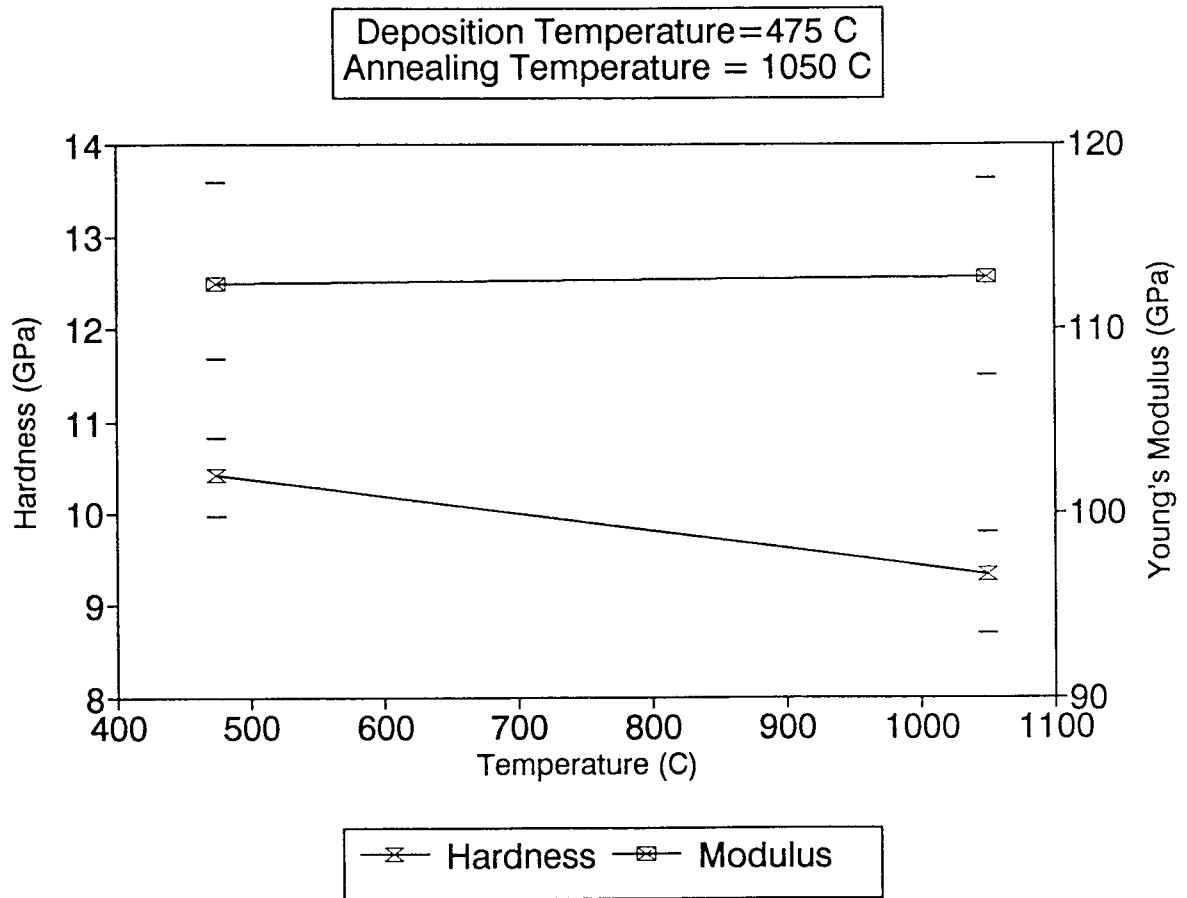


Figure 3.27 Annealing effect on the mechanical properties for film deposited at 475°C and annealed to 1050°C. After annealing, there was no detectable change on the Young's modulus while only slightly decrease on the hardness of the film.

3.10 Membranes Preparation

The preparation of membranes from the films deposited with high ratio of NH_3/TEAB (>10) at constant conditions of temperature (850°C) and pressure (0.5 torr) failed because these highly transparent, hydrogen-free films could not survive in KOH bath for a long etching time. It was also observed that the stress of these stoichiometric films was compressive, therefore, not suitable for fabrication of x-ray membranes. This problem was overcome by investigating the effect of incorporating silicon into the film.

Films deposited at constant temperature of 850°C , total pressure of 0.5 torr, and NH_3 flow rate of 350 sccm provide advantages of high optical transmission, hydrogen free, and relatively low depletion effect between wafers. Incorporated silicon in the films not only enhance the mechanical properties but also render the film stress from compressive nature to the desired tensile level, making this research much attractive. Membrane prepared with 1/5 ratio of HMDS/TEAB showed wrinkle on the surface. However, the boron silicon nitride membranes, 1 μm in thickness and 1.5 inches in diameter, were successfully made from the films deposited with the 1/4 ratio of HMDS/TEAB.

CHAPTER 4

CONCLUSIONS

Stoichiometric BN thin films were deposited on silicon and fused quartz wafers by low pressure chemical vapor deposition using ammonia and liquid precursor, borane-triethylamine complex (TEAB), at a constant temperature of 850°C and pressure of 0.5 torr. These films were found to be hydrogen-free and optically transparent; however, the stress was found to be compressive and the mechanical properties, such as hardness and modulus, were found to be inferior, thus, limited the films use as membrane materials for x-ray mask substrates.

Incorporation of silicon into the BN films by the precise control of the ratio of TEAB and HMDS in the precursor mixture had a promising effect on the stress and the mechanical properties. Boron silicon nitride membranes, 1 μm in thickness and 1.5 inches in diameter, were prepared by the two-step process. These membranes were found to be of high optical transparency and mechanical strength, absence of hydrogen, and adjustable tensile stress. As a result, these membranes were considered to be suitable materials as mask substrates for x-ray lithographic applications.

REFERENCES

1. Wolf, S., and R. N. Tauber. "Lithography 1: Optical Photoresist Materials and Process Technology." *Silicon Processing for the VLSI Era Volume 1* (1990): 407.
2. Fuller, G. E. "Optical Lithography Status." *Solid State Technology* (Sep. 1987): 113-118.
3. Sze, S. M. "Lithography." *VLSI technology* (1988): 141-176.
4. Paturi, V. "Synthesis and Characterization of Boron Nitride Masks for X-ray Lithography." Masters Thesis, NJIT (1991).
5. Heuberger, A. "X-ray Lithography." *J. Vac. Sci. Technol. B* 6 (1988): 107-121.
6. Brors, D. L. "X-ray Mask Fabrication." *SPIE* 333 (1982): 111-113.
7. Luthje, H. "X-ray Lithography for VLSI." *Philips Tech. Rev.* 41 (1983): 150-163.
8. Broers, A. N. "Fine-Line Lithography." R. A. Levy (ed.) *Microelectronic Materials and Processes* (1986): 409-419.
9. Nakamura, K. "Preparation and Properties of Boron Nitride Films by Metal Organic Chemical Vapor Deposition." *J. Electrochem. Soc.* 133 (1986): 1120-1123.
10. King, P., L. Pan, and P. Pianetta. "X-ray Induced Damage in Boron Nitride, Silicon, and Silicon Nitride Lithography Masks." *SPIE* 773 (1987): 126-131.
11. Wolf, S., and R. N. Tauber. "Advanced Lithography." *Silicon Processing for the VLSI Era Volume 1* (1990): 504-510.
12. Kern, W. "Chemical Vapor Deposition." R. A. Levy (ed.) *Microelectronic Materials and Processes* (1986): 203-246.
13. Rosler, R. S. "Low Pressure CVD Production Processes for Poly, Nitride, and Oxide." *Solid State Technol.* (Apr. 1977): 63-70.

14. Schmolla, W., and H. L. Hartnagel. "Amorphous BN Films Produced in a Double-Plasam Reactor for Semiconductor Applications." *Solid-State Electronics* 26 (1983): 931-939.
15. Gafri, O., A. Grill, and D. Itzhak. "Boron Nitride Coatings on Steel and Graphite Produced with a Low Pressure P. F. Plasma." *Thin Solid Films* 72 (1980): 523-527.
16. Hirayama, M., and K. Shohno. "CVD-BN for Boron Diffusion in Si and Its Application to Si Devices." *J. Electrochem. Soc.* 122 (1975): 1671-1676.
17. Matsumoto, O., M. Sasaki, H. Suzuki, H. Seshimo, and H. Uyama. "Deposition of Boron Nitride in a Microwave Discharge." *Department of Chemistry, Aoyama Gakuin University, Tokyo, Japan.*
18. Hanlon, L., M. Greenstein, W. Grossman, and A. Neukermans. "Electron Window Cathode Ray Tube Applications." *J. Vac. Sci. Technol. B* 4 (1986): 305-309.
19. Guzman, L., F. Marchetti, L. Calliari, I. Scotoni, and F. Ferrari. "Formation of BN by Nitrogen Ion Implantation of Boron Deposits." *Thin Solid Films* 117 (1984): L63-L66.
20. Weissmantel, C. "Ion Beam Deposition of Special Film Structures." *J. Vac. Sci. Technol.* 18 (1981): 179-185.
21. Rand, M. J., and J. F. Roberts. "Preparation and Properties of Thin Film Boron Nitride." *J. Electrochem. Soc.* 115 (1968): 423-429.
22. Hickernell, F. S. "Radio Frequency Sputter Deposited Boron Nitride Films." *J. Vac. Sci. Technol. A* 2 (1984): 322-325.
23. Satou, M., and F. Fujimoto. "Formation of Cubic Boron Nitride Films by Boron Evaporation and Nitrogen Ion Beam Bombardment." *J. Appl. Phys.* 22 (1983): L171-L172.
24. Halverson, W. "Effects of Charge Neutralization on Ion-Beam-Deposited Boron Nitride Films." *J. Vac. Sci. Technol. A* 3 (1985): 2141-2146.
25. Murarka, S. P., C. C. Chang, D. N. K. Wang, and T. E. Smith. "Effect of Growth Parameters on the CVD of Boron Nitride and Phosphorus-Doped Boron Nitride." *J. Electrochem. Soc.* 126 (1979): 1951-1957.

26. Williams, D. S., "Elastic Stiffness and Thermal Expansion Coefficient of Boron Nitride Films." *J. Appl. Phys.* 57 (1985): 2340-2343.
27. Yamada, M., M. Nakaishi, and K. Sugishima. "Improvements of Stress Controllability and Radiation Resistance by Adding Carbon to Boron-Nitride." *J. Electrochem. Soc.* 137 (1990): 2242-2246.
28. Shanfield S., and R. Wolfson. "Ion Beam Synthesis of Cubic Boron Nitride." *J. Vac. Sci. Technol. A* 1 (1983): 323-325.
29. Wada, T., N. Yamashita. "Formation of cBN Films by Ion Beam Assisted Deposition." *J. Vac. Sci. Technol. A* 10 (1992): 515-520.
30. Hyder, S. B., and T. O. Yep. "Structure and Properties of Boron Nitride Films Grown by High Temperature Reactive Plasma Deposition." *J. Electrochem. Soc.* 123 (1976): 1721-1725.
31. Dana, S. S., and J. R. Maldonado. "Low Pressure Chemical Vapor Deposition Boro-Hydro-Nitride Films and Their Use in X-Ray Masks." *J. Vac. Sci. Technol. B* 4 (1986): 235-239.
32. Levy, R. A., D. J. Resnick, R. C. Frye, and A. W. Yanof. "An Improved Boron Nitride Technology for Synchrotron X-Ray Masks." *J. Vac. Sci. Technol. B* 6 (1988): 154-161.
33. Johnson, W. A., R. A. Levy, D. J. Resnick, T. E. Saunders, and A. W. Yanof. "Radiation Damage Effects in Boron Nitride Mask Membranes Subjected to X-Ray Exposures." *J. Vac. Sci. Technol. B* 5 (1987): 257-261.
34. King, P. L., L. Pan, and P. Pianetta. "Radiation Damage Effects in Boron Nitride X-Ray Lithography Masks." *J. Vac. Sci. Technol. B* 6 (1988): 162-166.
35. Adams, A. C., and C. D. Capio. "The Chemical Deposition of Boron-Nitrogen Films." *J. Electrochem. Soc.* 127 (1980): 399-405.
36. Advanced Semiconductor Materials America, INC. "Micro 3 Manual"
37. Singh, R. N. "LPCVD of Boron Nitride from &-Trichloroborazine." *General Electric Company, N.Y.*

38. Nakamura, K. "Preparation and Properties of Amorphous Boron Nitride Films by Molecular Flow Chemical Vapor Deposition." *J. Electrochem. Soc.* 132 (1985): 1757-1762.
39. Miyamoto, H., M. Hirose, and Y. Osaka. "Structural and Electronic Characterization of Discharge-Produced Boron Nitride." *Jap. J. Appl. Phys.* 22 (1983): L216-L218.
40. Takahashi, T., H. Itoh, and M. Kuroda. "Structure and Properties of CVD-BN Thick Film Prepared on Carbon Steel Substrate." *J. Crystal Growth* 53 (1981): 418-422.
41. Takahashi, T., H. Itoh, and A. Takeuchi. "Chemical Vapor Deposition of Hexagonal Boron Nitride Thick Film on Iron." *J. Crystal Growth* 47 (1979): 245-250.
42. Fukumoto, H., and T. Hamada. "Scanning Tunneling Microscopy of Hexagonal BN Grown on Graphite." *J. Appl. Phys.* 69 (1991): 8076-8078.
43. Montasser, K., and S. Hattori. "Characterization of Hard Transparent B-C-N-H Thin Films Formed by Plasma Chemical-Vapor Deposition at Room Temperature." *J. Appl. Phys.* 58 (1985): 3185-3189.
44. Shih, K. T. "Synthesis and Characterization of Silicon Nitride Film Deposited by Plasma Enhanced Chemical Vapor Deposition from Ditertiary-butyl Silane." Masters Thesis, NJIT (1991).